Correlated quantum phenomena in the strong spin-orbit regime

William Witczak-Krempa

Perimeter Institute for Theoretical Physics, Waterloo, Ontario N2L 2Y5, Canada

Gang Chen

Department of Physics, University of Colorado, Boulder, Colorado, US

Yong Baek Kim

Department of Physics, University of Toronto,
Toronto, Ontario M5S 1A7, Canada and
School of Physics, Korea Institute for Advanced Study, Seoul 130-722, Korea

Leon Balents

Kavli Institute of Theoretical Physics, University of California,
Santa Barbara, Santa Barbara, CA, 93106

We discuss phenomena arising from the combined influence of electron correlation and spin-orbit coupling, with an emphasis on emergent quantum phases and transitions in heavy transition metal compounds with $4d$ and $5d$ elements. A common theme is the influence of spin-orbital entanglement produced by spin-orbit coupling, which influences the electronic and magnetic structure. In the weak-to-intermediate correlation regime, we show how non-trivial band-like topology leads to a plethora of phases related to topological insulators. We expound these ideas using the example of pyrochlore iridates, showing how many novel phases such as the Weyl semi-metal, axion insulator, topological Mott insulator, and topological insulators may arise in this context. In the strong correlation regime, we argue that spin-orbital entanglement fully or partially removes orbital degeneracy, reducing or avoiding the normally ubiquitous Jahn-Teller effect. As we illustrate for the honeycomb lattice iridates and double perovskites, this leads to enhanced quantum fluctuations of the spin-orbital entangled states and the chance to promote exotic quantum spin liquid and multi-polar ordered ground states. Connections to experiments, materials, and future directions are discussed.

CONTENTS

I. INTRODUCTION

The subject of this review is the combination of two central threads of quantum materials research. The first, correlated electron physics, is a venerable but still vibrant subject, born from observations of Mott, Hubbard, Anderson, and others on the properties of $3d$ transition metal oxides. It is largely concerned with the diverse properties of electronic materials which are insulating, or in the process of becoming so, as a result of electron-electron interactions,[1,2] most importantly the strong local Hubbard repulsion U between electrons occupying the same orbital. A plethora of phenomena arises from correlated electron physics, including local moment formation and magnetism, correlated metallic states, quantum criticality, and unconventional superconductivity.[2] The second thread, non-trivial physics from strong spin-orbit coupling (SOC), includes a body of work on f-electron materials[3] and the much more recent activity begun with the theoretical proposal of

topological insulators (TIs) in 2005.[4–6] SOC is a relativistic effect, which provides an interaction between the orbital angular momentum and electron spin in atoms, and is usually considered a small perturbation in the discussion of electrons in solid. However, in heavy elements it need not be weak – it effectively increases proportionally to Z^4, where Z is the atomic number – and indeed has striking qualitative effects. Since 2005, the investigation of topological aspects of electron bands has exploded, both theoretically and experimentally.[4–6] From the materials perspective, the domain of the TI field has mostly been the class of solids with heavy s- and p-electron elements such as Bi, Pb, Sb, Hg, and Te. In these materials, topologically protected Dirac-like surface states have been predicted and observed, and a host of further phenomena are currently under intense investigation.

The two research strands come together in the heavy transition metal compounds drawn especially from the $5d$ series, and in some cases the $4d$'s as well. Upon descending the periodic table from the $3d$ to $4d$ to $5d$ series, there are several competing trends. First, the d orbitals become more extended, tending to reduce the electronic repulsion U and thereby diminish correlation effects. However, simultaneously, the SOC increases dramatically, leading to enhanced splittings between otherwise degenerate or nearly degenerate orbitals and bands, reducing in many cases the kinetic energy. The latter effect can offset the reduction in U, allowing correlation physics to come into play.

It is instructive to consider a generic model Hamiltonian describing the above discussion:

$$H = \sum_{i,j;\alpha\beta} t_{ij,\alpha\beta} \; c_{i\alpha}^\dagger c_{j\beta} + \text{h.c.} + \lambda \sum_i \boldsymbol{L}_i \cdot \boldsymbol{S}_i + U \sum_{i,\alpha} n_{i\alpha}(n_{i\alpha} - 1) \; , \tag{1}$$

where $c_{i\alpha}$ in the annihilation operator for an electron in orbital α at site i and $n_{i\alpha} = c_{i\alpha}^\dagger c_{i\alpha}$, the corresponding occupation number, t the hopping amplitude, λ the atomic SOC entangling spin ($\boldsymbol{S}_i$) and angular momentum ($\boldsymbol{L}_i$), and U the Hubbard repulsion. An explicit example of the spin-orbital entanglement due to λ is given later in Eq. (3). We have for simplicity omitted the Hunds interaction between spins in different orbitals on the same site, which is much smaller than U but can sometimes have significant effects[7] - it is, however, unimportant in the specific examples discussed in detail in this review. A schematic "phase diagram" can be drawn as in Figure 1 in terms of the relative strength of the interaction U/t and the SOC λ/t.[8] We emphasize this is schematic, in part because the problem is unsolved, and in part because Eq. (1) can represent many different physical situations by the choice of orbitals and lattice/band structure encoded in $t_{ij,\alpha\beta}$, and the ground states which occur certainly depend upon these choices. In this diagram, two lines (which are not meant necessarily as sharp boundaries but rather as demarcating different limits) divide the weak and strong correlation regions, and the weak and strong SOC regimes, thereby generating four quadrants. Conventional transition metal materials reside on the left hand side of the diagram, where SOC is weak $\lambda/t \ll 1$, and a conventional metal-insulator transition (MIT) may occur when U is comparable to the bandwidth, or a few times t. Upon increasing SOC, when

$U/t \ll 1$, a metallic or semi-conducting state at small U may be converted to a semi-metal or to a TI. What happens when both SOC and correlations are present? Several arguments suggest that λ and U tend to cooperate rather than compete, in generating insulating states. Including SOC first, we have already remarked upon the splitting of degeneracies and the consequent generation of multiple narrow bands from relatively mixed ones. The narrow bands generated by SOC are more susceptible to Mott localization by U, which implies that the horizontal boundary in Figure 1 shifts downward with increasing λ. If we include correlations first, the U tends to localize electrons, diminishing their kinetic energy. Consequently the on-site SOC λ, which is insensitive to or even reduced by *delocalization*, is relatively enhanced. Indeed, in the strong Mott regime $U/t \gg 1$, one should compare λ with the spin exchange coupling $J \propto t^2/U$, rather than t. As a result, the vertical boundary shifts to the left for large U/t. We see that there is an intermediate regime in which insulating states are obtained only from the combined influence of SOC and correlations – these may be considered *spin-orbit assisted Mott insulators*. Here we are using the term "Mott insulator" to denote any state which is insulating by virtue of electron-electron interactions. In Sec. IV, we will remark briefly on a somewhat philosophical debate as to what should "properly" be called a Mott insulator.

Terminology aside, an increasing number of experimental systems have appeared in recent years in this interesting correlated SOC regime. Most prolific are a collection of *iridates*, weakly conducting or insulating oxides containing iridium, primarily in the Ir^{4+} oxidation state. This
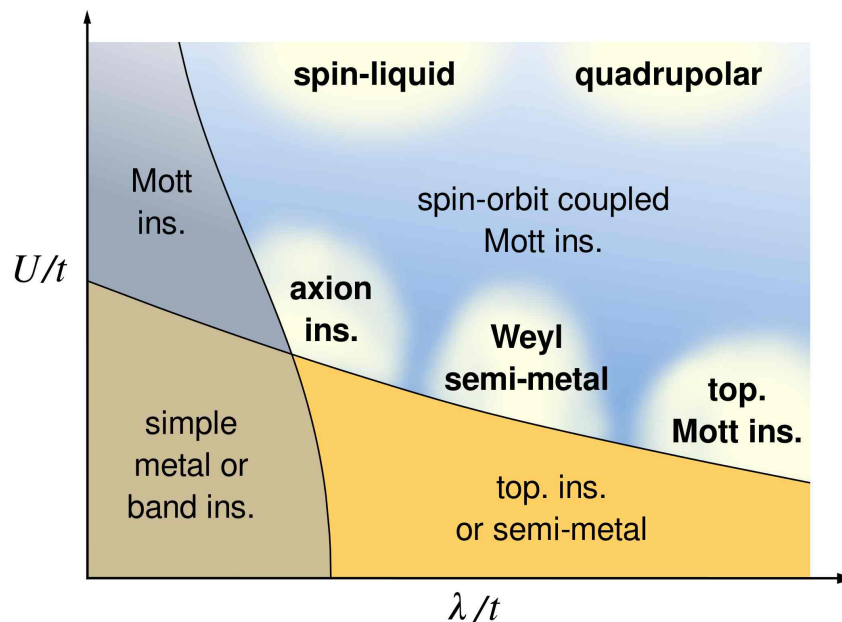

FIG. 1. Sketch of a generic phase diagram for electronic materials, in terms of the interaction strength U/t and SOC λ/t. The materials in this review reside on the right half of the figure.

includes a Ruddlesdon-Popper sequence of pseudo-cubic and planar perovskites $Sr_{n+1}Ir_nO_{3n+1}$ ($n = 1, 2, \infty$),[9–16] hexagonal insulators $(Na/Li)_2IrO_3$,[17–22] a large family of pyrochlores, $R_2Ir_2O_7$,[23–25] and some spinel-related structures.[26,27] Close to iridates in the periodic table are several osmium oxides such as $NaOsO_3$[28] and $Cd_2Os_2O_7$,[29] which experimentally display MITs. Apart from these materials where the microscopic SOC is truly rather strong ($\lambda \approx 0.4$eV), there are also examples which arise in materials further "up" in Figure 1, in which electrons are strongly localized, the competing exchange scale is anomalously weak, making even smaller SOC "strong". This includes the spin-orbital liquid material $FeSc_2S_4$,[30–32] possibly the single layer vanadate Sr_2VO_4,[33] and a host of double perovskites, $A_2BB'O_6$,[34–47] where the exchange scale is small because the electronically active B' ions are well separated spatially. For space reasons, we cannot discuss all of these materials, but will take examples from this list as illustrations.

This review is organized based on a consideration of two limits within this domain: the weak-to-intermediate correlation regime, $U/W \lesssim 1$, where W is the bandwidth which is typically a few times t, and the strong Mott limit, $U/W \gg 1$, both in the presence of strong SOC. Conceptually, in the former, the electrons remain delocalized enough that band or band-like topology continues to play an important role, as in the case of TIs.[4–6] Notably, interactions open up possibilities for new types of topological phases. This includes Weyl semi-metals (WSM) with Dirac-like bulk quasiparticles and surface "Fermi-arc" states,[48–51] or axion insulators with unusual electromagnetic response,[52,53] which can arise in the presence of spontaneous magnetic order. Phase transitions between these states,[8,49–54] and amongst metals and insulators, also occur in this regime, and yet more exotic phases have also been envisioned.[8,55] We discuss this weak to intermediate correlation regime in Sec. II, taking the pyrochlore iridates, $R_2Ir_2O_7$, as primary experimental examples.

In the strong Mott regime, discussed in Sec. III, electron band topology no longer plays a role, since electronic states are not extended. However, SOC still offers new physics by fully or partially lifting orbital degeneracy of partially filled d shells, not by ordering orbitals, but by *entangling* the orbital and spin degrees of freedom.[32,56,57] This provides a distinct mechanism to avoid the Jahn-Teller effect and classical orbital ordering. The orbital degeneracy may be fully lifted by SOC, which occurs in iridates in the strong Mott+SOC limit, or partially lifted, which is the case for many d^1 or d^2 ions. In this review we illustrate both possibilities, taking the honeycomb iridates,[17–22] Na_2IrO_3 and Li_2IrO_3, as examples of the former, and double perovskites,[34–47] as examples of the latter. In either case, the strong SOC results in strongly anisotropic exchange interactions, and for the case of partial degeneracy lifting, these have a highly non-trivial *multi-polar* nature.[56,57] We describe how these unusual interactions can promote large quantum fluctuations and lead to novel quantum ground states that are not possible without strong SOC.[56–58] In particular, quantum spin liquid and quadrupolar (spin nematic) ordered phases have been suggested to occur in these systems.

Table I summarizes the emergent phases encountered in this review. The theoretical and experimental status of the weak-intermediate and strong correlation regimes are presented in Sections II and III, respectively. Following this, we conclude the review with a discussion of open issues and

TABLE I. Emergent quantum phases in correlated spin-orbit coupled materials. All phases have U(1) particle-conservation symmetry – *i.e.* superconductivity is not included. Abbreviations are as follows: TME = topological magnetoelectric effect, TRS = time reversal symmetry, P = inversion (parity), (F)QHE = (fractional) quantum Hall effect, LAB = Luttinger-Abrikosov-Beneslavskii.[59] Correlations are W-I = weak-intermediate, I = intermediate (requiring magnetic order, say, but mean field-like), and S = strong. $[A/B]$ in a material's designation signifies a heterostructure with alternating A and B elements.

Phase	Symm.	Correlation	Properties	Proposed materials
Topological Insulator	TRS	W-I	Bulk gap, TME, protected surface states	many
Axion Insulator	P	I	Magnetic insulator, TME, no protected surface states	$R_2Ir_2O_7$, $A_2Os_2O_7$
WSM	Not both TRS & P	W-I	Dirac-like bulk states, surface Fermi arcs, anomalous Hall	$R_2Ir_2O_7$, $HgCr_2Se_4$, $\ldots$
LAB Semi-metal	cubic + TRS	W-I	Non-Fermi liquid	$R_2Ir_2O_7$
Chern Insulator	broken TRS	I	Bulk gap, QHE	$Sr[Ir/Ti]O_3$, $R_2[B/B']_2O_7$
Fractional Chern Insulator	broken TRS	I-S	Bulk gap, FQHE	$Sr[Ir/Ti]O_3$
Fractional Topological Insulator, Topological Mott Insulator	TRS	I-S	Several possible phases. Charge gap, fractional excitations	$R_2Ir_2O_7$
Quantum spin liquid	any	S	Several possible phases. Charge gap, fractional excitations	$(Na,Li)_2IrO_3$, Ba_2YMoO_6
Multipolar order	various	S	Suppressed or zero magnetic moments. Exotic order parameters.	$A_2BB'O_6$

other materials in Sec. IV.

II.   WEAK TO INTERMEDIATE CORRELATIONS

Following the discovery of topological insulators[4,5] (TIs), it is now recognized that SOC is an essential ingredient in forming certain topological phases. The TI is characterized by a $\mathbb{Z}_2$ topological invariant, which may be obtained from the band structure, in the presence of time-reversal symmetry (TRS). This phase has a bulk excitation gap, but is distinguished from trivial band insulators by the presence of protected metallic surface states. The non-trivial bands in

the TI must "unwind" upon crossing the interface with a time-reversal preserving vacuum or a trivial band insulator, leading to the closing of the excitation gap and a conducting state at the interface. Stemming as it does from band structure considerations, the TI relies upon some degree of itineracy. Other TI-related phases with gapless nodes – point Fermi surfaces – in the bulk have also been explored theoretically, and obviously also require delocalized electronic states.

In this section, we discuss phenomena involving band-like topology in the presence of interactions. Non-trivial band topology can probably only arise when correlations are not so strong as to localize electrons fully to single atoms. Consequently, we focus on this regime of weak to intermediate correlations. From the theoretical point of view, this means that a Hubbard model, rather than one of localized spins, is likely a better starting point.

What new phenomena can be expected, relative to the uncorrelated s- and p-electron materials which are the mainstay of TI experiments? TIs obviously are stable to interactions, and quantitatively, correlations may even increase the gap in some cases (With correlations, in contrast to the free case, the surface states have the potential of spontaneously breaking TRS or even exhibiting exotic fractionalization[60]). A more qualitatively novel prospect is to probe topological phases with spontaneous time-reversal breaking, since magnetism is common in correlated materials. In general, the $\mathbb{Z}_2$ classification fails for time-reversal broken systems, and instead Chern insulators, *i.e.* materials with quantized Hall effects, may occur for instance. In the presence of crystalline symmetries, notably inversion, a $\mathbb{Z}_2$ index may reappear.[49,61–65] This is the case in the "axion insulator",[49,62,63] which may be characterized by a quantized magnetoelectric effect, *i.e.* an electric polarization $\boldsymbol{P}$ can be generated by applying a magnetic field $\boldsymbol{B}$: $\boldsymbol{P} = \frac{\theta}{(2\pi)^2}\boldsymbol{B}$ with $\theta = \pi$ such that the ratio P/B is universal and quantized. In fact the same is true for three-dimensional TIs, and the quantized magnetoelectric effect can be used to define TIs[66] and axion insulators[53,67,68] in the presence of interactions.

Non-trivial topology can also appear in gapless phases, such as in the WSM.[48,49,69] At the level of band theory, the WSM has a Fermi surface consisting of points, where only two bands meet linearly, see Figure 2. This implies that either TRS or inversion is broken, for otherwise all bands would be two-fold degenerate. In this review, we will encounter examples arising from a spontaneous breaking of TRS at sufficiently large U. The band touchings of the WSM are three-dimensional analogs of the massless Dirac fermions in clean graphene. However, contrary to the latter, they should be regarded as topological objects – monopoles or hedgehogs in momentum space – because they act as sources of the momentum space Berry flux.[48,49,69,70] Consequently, they always come in pairs with opposite chiralities, corresponding to a positive or negative monopole charge, as illustrated in Figure 2. An isotropic example of a Weyl fermion is given by the following Bloch Hamiltonian (we take the touching to be at $\boldsymbol{k}_W$)

$$\mathcal{H}(\boldsymbol{k}) = \pm v(\delta k_x \sigma_x + \delta k_y \sigma_y + \delta k_z \sigma_z)\,, \quad \delta \boldsymbol{k} = \boldsymbol{k} - \boldsymbol{k}_W \qquad (2)$$

where $\pm$ corresponds to positive/negative chirality and σ_i are the Pauli matrices acting on the space
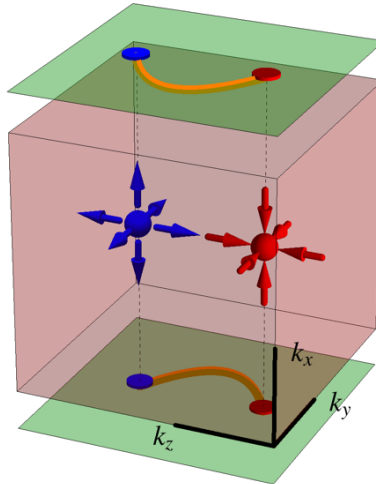
(a)

FIG. 2.   Two opposite-chirality Weyl points in the three dimensional Brillouin zone (BZ), and the associated Fermi arc surface states. The green sheets correspond to the top and bottom surface-BZs. This minimal WSM must break TRS, and will have a corresponding anomalous quantum Hall conductivity, $\sigma_{xy} = (e^2/2\pi h)\Delta k$, where Δk is the momentum-space separation between the two Weyl points.

of the two non-degenerate bands touching at the Weyl point. Because any local perturbation is a combination of Pauli matrices, it can only move the touching in the Brillouin zone (BZ) and not lift it, since all σ_i already appear in $\mathcal{H}$. As a consequence of the non-trivial bulk topology, the WSM hosts non-trivial surface states on certain boundaries, which take the form of open Fermi arcs,[49] as shown in Figure 2(a). This cannot occur in a purely 2D system, just like the existence of an odd number of Dirac fermions at the surface of a three-dimensional $\mathbb{Z}_2$ TI, which apparently violates the "fermion doubling" theorem.[71] In both cases, however, the "partner" electronic states exist on the opposite surface, which elegantly resolves the apparent paradox. For some further discussion of WSMs, including other realizations,[51,72,73] and of generalizations of these ideas to superconductors,[74] we refer readers to recent reviews.[75,76]

The Chern insulator, axion insulator, and WSM require interactions to produce magnetic order, but once produced, a mean field description in terms of a static exchange field suffices, and the electronic quasiparticles are consequently weakly correlated. Other phases arising in interacting systems with strong SOC may be more intrinsically correlated. Several interacting analogs of TIs have been envisioned, which are not adiabatically connected to the ground states of *any* non-interacting electron Hamiltonian, with or without broken symmetries. These include the topological Mott insulator of Ref. 8, which exhibits *spin-charge separation* and TI-like surface states composed of neutral fermions, and *fractional* Chern insulators[77–79] which display a fractional quantum Hall effect without an external magnetic field. Presently, while we believe the *ingredients* for these sorts of phases are present in the class of materials discussed in this review, a direct

connection of specific compounds to specific states of this type is an open theoretical challenge.

A final category of phenomena to be mentioned in the intermediate correlation regime are thermal and quantum *phase transitions*. The elephant in the room is the MIT itself, whose character in the strong SOC limit has been very little investigated, but may be very different from what has been observed in traditional $3d$ compounds. For example, theory has established that the MIT may occur through an intermediate WSM state, and transitions to/from WSM states may be studied. Other types of correlation-driven MITs have been suggested. Note that at $T > 0$, the difference between a metal and an insulator is quantitative not qualitative (since $\sigma \neq 0$ always), so that the evolution from a metal to an insulator at $T > 0$ needs not coincide with any phase transition. The onset of magnetic order in correlated metals and insulators constitutes another type of criticality. Such transitions may again be affected by strong SOC.

A. Pyrochlore iridates

In this section we expand on the theory and experimental status of new phases and transitions in the context of the pyrochlore iridates, $R_2Ir_2O_7$ (R-227) where R is a rare earth element. We choose these compounds because they comprise a large family for which experiments have revealed thermal phase transitions and an evolution from metallic to insulating states, and largely systematic variation of properties with R. Many key theoretical ideas in the field have also been introduced in this context, including topological Mott insulators,[8,55,80] chiral spin liquids,[81] WSMs,[49,50] and axion insulators.[49,53] This has contributed to a substantial experimental effort,[23,24,82–94] in particular to determine the nature of the elusive magnetic ordering. We shall first review the experimental knowledge of the pyrochlore iridates, and will then describe the theoretical work they have motivated.

1. Experimental resume

The structure of these materials is well established, consisting of interpenetrating pyrochlore nets for both the rare earth and iridium ions.[23,95] Each such lattice can be described as a face centered cubic (fcc) Bravais lattice with four sites per unit cell forming a tetrahedron. The crystal structure is illustrated in Figure 3. The fcc lattice constant was found to range from $a = 1.01$ to 1.04 nm,[23,85,91] depending on the R element. Another important structural parameter is the oxygen x-parameter, which determines the symmetry of the oxygen environment around each Ir cation: when $x = x_{ideal} = 5/16 = 0.3125$ the oxygens form a perfect octahedron around each Ir. Otherwise, the oxygen octahedron becomes elongated ($x < x_{ideal}$) or compressed ($x > x_{ideal}$) along the [111] directions. These distortions are called trigonal because they preserve three-fold rotational symmetries. Experiments show that the pyrochlore iridates all have compressed octahedra.[82,91]

Let us first review the temperature dependence of the resistivity, ρ. All members of the family
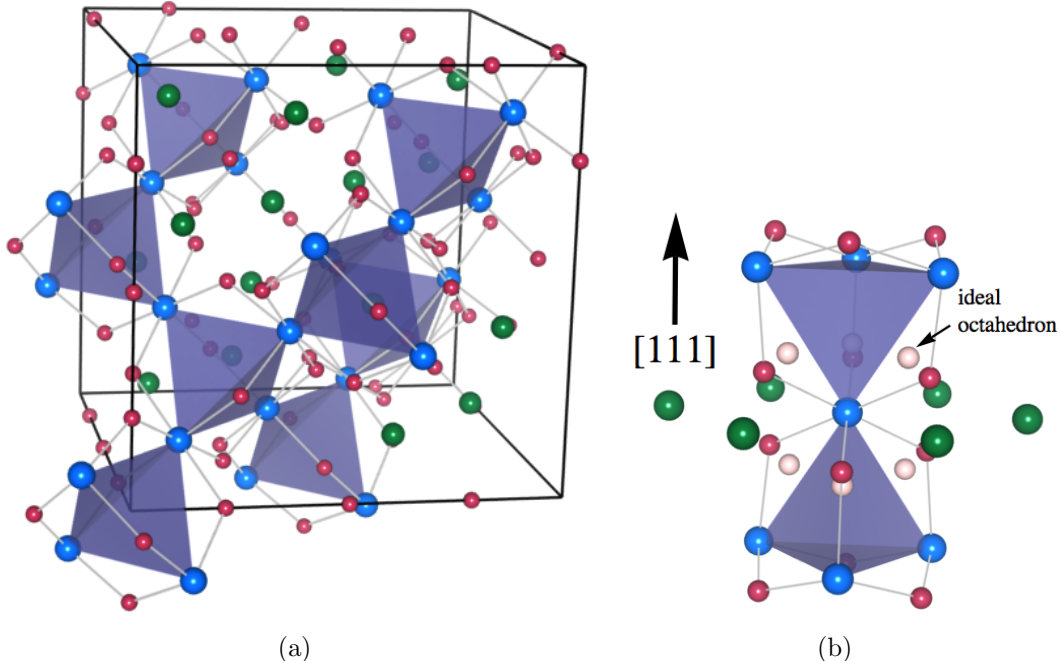
FIG. 3. Pyrochlore lattice structure showing the Ir (blue) tetrahedra. Trigonally compressed cages of oxgyens (small & red) surround each Ir. The rare earth R ions are in green. The box is aligned along the [100], [010] and [001] directions. In b), the light spheres would correspond to the position of oxygen ions in an ideal octahedron, expected for a larger R^{3+} ion. All pyrochlore iridates show trigonal compression of the oxygen cages along the [111] directions.

show a diverging ρ at sufficiently low temperature, except Pr-227.[23,24,84] For the compounds with a larger R^{3+} ion such as Eu-, Sm- and Nd-227 the resistivity goes from being "metallic" ($d\rho/dT > 0$) at large temperatures $T > T_c$ to "non-metallic" ($d\rho/dT < 0$) at smaller temperatures $T < T_c$. This is illustrated for Eu-227 in Figure 4(a). Pr-227 lies at the end of the spectrum in that it has the largest ionic radius, and does not show a major resistivity upturn down to the lowest temperatures, in agreement with the above trend. For compounds with smaller R^{3+} ions such as for $R =$ Lu, Yb, Ho, Y, etc the slope does not change sign and the resistivity is "non-metallic" throughout. In that case, the upturn at T_c is smoother. One can tentatively explain this trend according to which a larger R^{3+} cation leads to a more metallic ρ as follows: Larger R^{3+} ions lead to a decreased trigonal compression of the octahedra (Figure 3(b)), which increases the Ir-O orbital-overlap and thus facilitates the hopping of the Ir electrons.[96]

A variety of sharp features in the magnetic properties occur at the same temperature as the resistivity upturn, T_c, which support its interpretation as a true phase transition. Most notably, the field cooled (FC) and zero-field cooled (ZFC) magnetic susceptibilities branch away from each other,[24,82] as shown in Figure 4(a) for Eu-227. In addition, μSR experiments, which have been performed on Eu-,[86] Nd-,[92,97] Yb-,[93] and Y-227,[93] show the continuous rise of a well-defined muon-precession frequency directly below T_c (illustrated in Figure 4(a) for Eu-227). This is indicative of
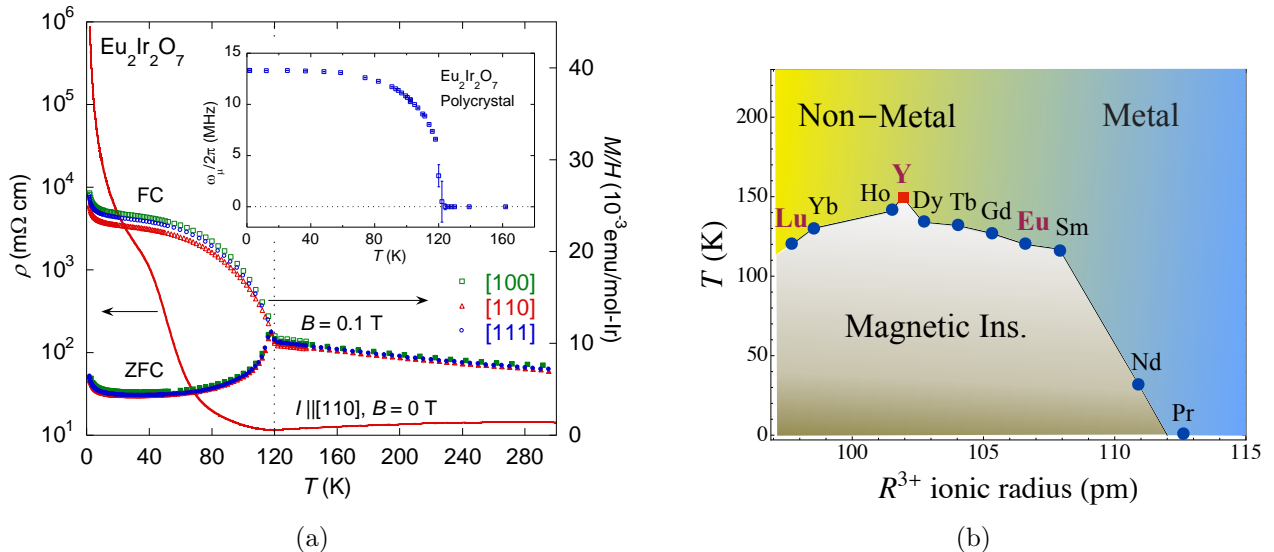
FIG. 4. a) The main panel shows the resistivity, and field cooled (FC) and zero field cooled (ZFC) susceptibilities for Eu-227, while the insert the spontaneous muon oscillation frequency. Data adapted from Refs. 86 and 87. b) Phase diagram for the pyrochlore iridates R-227 based on transport and magnetism measurements. (This is a supplemented and modified version of the diagram found in Ref. 84.) The R-elements that do not have a local magnetic moment are emphasized in bold magenta. The only non-lanthanide, $R = Y$, is denoted by a square.

long-range magnetic ordering into a commensurate structure. However, due to difficulties in performing neutron scattering experiments on Ir-based compounds, the precise nature of the ordering remains unknown. Nevertheless, it has been inferred that a *second-order* phase transition to an AF insulator occurs at T_c. Ferromagnetism can be largely ruled out by the absence of magnetic hysteresis.[23,82] The second order nature of the transition is further supported by the presence of peaks in the heat capacity at T_c.[24,84] The essence of the experimental observations on the pyrochlore iridates is summarized in the phase diagram Figure 4(b).

2. Electronic structure

The basic element of the description of these materials is the iridium electronic structure. We will neglect for the most part the rare earth magnetism, which plays a role in some (but not all) of the compounds at very low temperature. Following the analysis of the Ir-electron physics, we will briefly examine their interplay with local moments in Section II A 5.

We begin by examining the local atomic physics associated with the Ir cations. The outer-shell electrons of Ir^{4+} are in a $5d^5$ configuration, half-filling the ten d-levels. The dominant crystal field splitting comes from the oxygen octahedra surrounding each Ir cation, which splits the levels into a higher energy e_g orbital doublet and a lower t_{2g} orbital triplet, spanned by orbitals with xy, yz and

zx symmetry. These are separated by a ~ 2 eV gap and as such we can neglect the higher energy e_g levels. We then must take into account both the SOC and trigonal distortions. Let us begin with atomic SOC in Ir^{4+} ions. The full angular momentum operator $\boldsymbol{L}$ projected to the t_{2g} manifold acts as an effective angular momentum one, $\boldsymbol{L}_{\text{eff}}$, up to a minus sign, *i.e.* $\mathcal{P}_{t2g}\boldsymbol{L}\mathcal{P}_{t2g} = -\boldsymbol{L}_{\text{eff}}$, where $\mathcal{P}_{t2g}$ represents the projection on the t_{2g} manifold. Therefore, the SOC λ splits the t_{2g} spinful manifold into a higher energy $J_{\text{eff}} = 1/2$ doublet and a lower $J_{\text{eff}} = 3/2$ quadruplet. The states in these multiplets exhibit spin-orbital entanglement. For example, the Jeff $= 1/2$ states are

$$|J_{\text{eff}}^z = +1/2\rangle = \frac{1}{\sqrt{3}}(|xy,\uparrow\rangle + |yz,\downarrow\rangle + i\,|zx,\downarrow\rangle)\,,$$
$$|J_{\text{eff}}^z = -1/2\rangle = \frac{1}{\sqrt{3}}(-|xy,\downarrow\rangle + |yz,\uparrow\rangle - i\,|zx,\uparrow\rangle)\,. \tag{3}$$

In an ionic picture, since Ir^{4+} has 5 d-electrons, the $J_{\text{eff}} = 1/2$ doublet is half-filled, and only this orbital is involved in the low energy electronic structure. More generally, if trigonal splitting is included, the $J_{\text{eff}} = 3/2$ levels are split and mixed with the $J_{\text{eff}} = 1/2$ ones. In the general case, there is a highest Kramers doublet, whose character varies with the ratio of SOC to trigonal splitting, between a $J_{\text{eff}} = 1/2$ doublet and a $S = 1/2$ one.

A band structure view is complementary to the ionic picture as we now discuss. If only the highest doublet is involved, we expect 4 two-fold degenerate bands near the Fermi energy, as there are 4 Ir per unit cell. As discussed by Wan *et al.*[49] and Yang *et al.*,[54] it is instructive to consider their structure at the Γ point. Due to cubic symmetry, the 8 Bloch states at this point decompose into 2 two-dimensional irreducible representations (irreps) and 1 four-dimensional irrep. By electron counting, these bands should be half-filled, so that if the order of these irreps, in terms of degeneracies, is 2-2-4 or 4-2-2, a band insulating state may occur, while if the order is 2-4-2, the 4-dimensional irrep must be half-filled and hence the system cannot be gapped at the band structure level (see the lowest panel of Figure 5(b)). The former situation was obtained by Ref. 8 based on a phenomenological but ad-hoc Hubbard model for small U. They found a transition from a semi-metallic ground state to a TI one with increasing the ratio of SOC to hopping. Subsequently, by *ab initio* methods, Wan *et al.* found[49] the latter, 2-4-2, ordering of irreps in Y-227. In this case, a TI is impossible, but other topological phases can occur with increasing correlations. For those iridates with metallic paramagnetic states, the 2-4-2 scenario may be more plausible.

A convenient tight-binding model which covers both limits was introduced in Ref. 50 and 98. It considers the minimal number of degrees of freedom, *i.e.* a single Kramers doublet per site, which leads to a total of 8 bands. One can show that the most general nearest-neighbor (NN) TRS Hamiltonian has the form[99]

$$H_0 = \sum_{\langle i,j\rangle} c_i^\dagger (t_1 + it_2 \boldsymbol{d}_{ij} \cdot \boldsymbol{\sigma}) c_j\,, \tag{4}$$

where the hopping parameters t_1 and t_2 are real, and $\boldsymbol{\sigma}$ is a vector of Pauli matrices acting on the pseudospin degree of freedom. The t_2 term generates non-trivial Berry phases for the hopping

electrons, and will play a key role in realizing topological phases. The real vector $\boldsymbol{d}_{ij}$ is aligned along the opposite bond of the tetrahedron containing i, j. Diagonalization of H_0 reveals a semi-metallic state with the 2-4-2 ordering when $-2 \leq t_2/t_1 \leq 0$, and a TI otherwise.[98,99] Notably, the semi-metallic state so obtained is not a compensated system with electron-hole pockets but a *zero gap semiconductor*. More recently it was argued that such a state forms a stable *non-Fermi liquid* phase with a quadratic band touching at the Γ point, christened a "Luttinger-Abrikosov-Beneslavskii" (LAB) phase for historical reasons.[59]

3. Magnetism and Weyl fermions

As discussed in Sec. II A 1, the experimental results strongly suggest antiferromagnetic order in the low-temperature insulating state of the iridates. This is also indicated from theory. LDA+U calculations by Wan *et al.* found an antiferromagnetic (AF) ground state with each spin oriented along its local trigonal axis and all spins on a given tetrahedron pointing in or out of that tetrahedron.[49] Such an "all-in/all-out" (AIAO) state, illustrated in Figure 5, maintains the unit cell and cubic symmetry of the lattice, and is consistent with the lack of any indication of structural transitions in experiment. The same AIAO state was obtained in a phenomenological Hubbard model, by theoretical methods of varying sophistication (Refs. 50, 53, 98, and 100).

In the magnetically ordered state, the broken TRS but preserved inversion symmetry admits the possibility of both WSM and axion insulator phases. Wan *et al.* indeed found a WSM phase for a range of U in their LDA+U calculations, and suggested but did not find an axion insulator state.[49] In fact, introduction of arbitrarily weak AIAO magnetic order converts the quadratic band touching LAB phase to a Weyl semi-metal,[50,98] which is illustrated in the middle panel of Figure 5(b). As remarked earlier, this phase is stable and indeed the Weyl points must migrate from the Γ point toward the zone boundary to pairwise annihilate before a true insulator is found at larger U. Such behavior was found by adding a Hubbard repulsion U to the tight-binding model of Eq. (4), within a Hartree-Fock approximation[50,98] (small second neighbor hopping is needed to obtain the generic linear dispersion relation in the WSM phase with AIAO order). This is illustrated in Figure 5. The quantitative width of the WSM in phase space varies between different calculations, and can be very narrow, owing to rather flat bands and the relatively fast growth of the local moment as the AIAO phase is entered. Other types of magnetic order, *e.g.* ferromagnetism, can also induce Weyl points, or relatives of them.[59,101]

Many signatures of the WSM have been suggested. We have already mentioned the surface Fermi arcs. Without disorder, the low frequency optical conductivity scales as $\sigma(\omega) \sim \omega$. Though a pair of opposite Weyl points mediates an intrinsic Hall conductivity,[70,102] this sums to zero given the cubic symmetry of the AIAO state, which dictates at least 8 nodes. However, it was suggested that a zero field Hall conductivity could be induced by appropriate strain.[102] Interesting transport phenomena are predicted, related to the Adler-Bell-Jackiw anomaly of Weyl fermions, in parallel electric and magnetic fields.[103] In general, taking into account the interplay of various types of
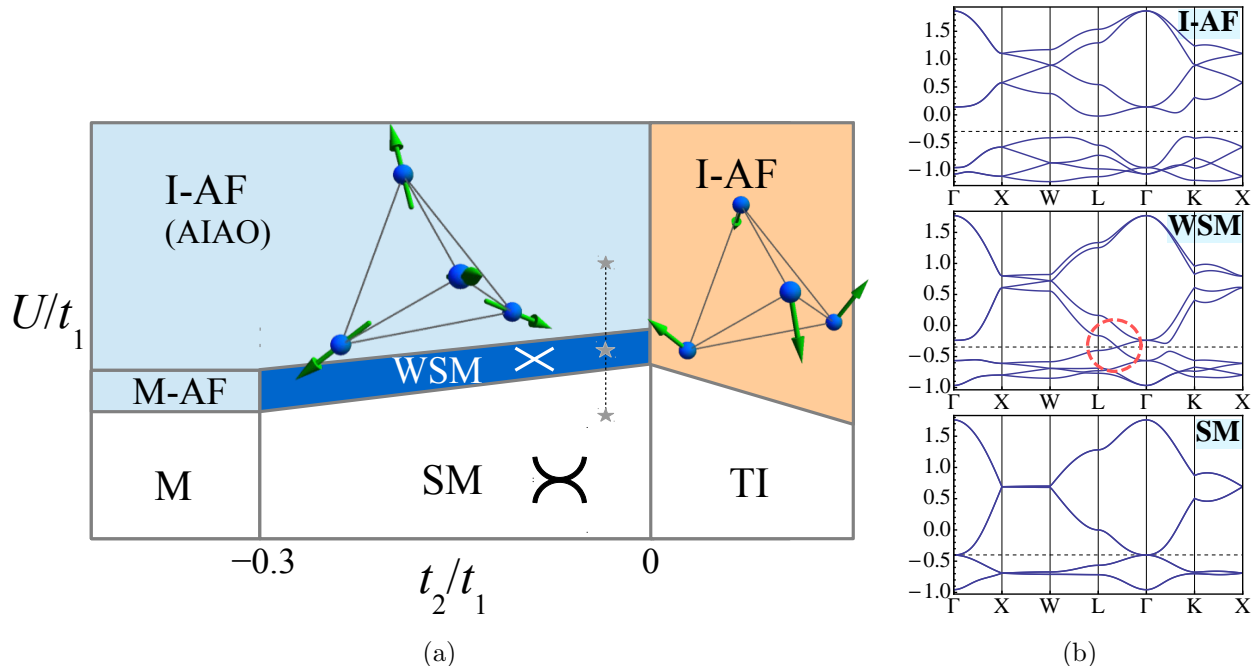
FIG. 5.   a) Schematic mean-field phase diagram of the Hubbard model on the pyrochlore lattice[50,98] (the kinetic Hamiltonian, Eq. (4), has been supplemented by small next nearest neighbor hopping). The shaded regions harbor antiferromagnetic (AF) order, which can be of the AIAO type (blue) or a related type (orange). M = Metal, I/M-AF= Insulating/Metallic AF. b) The evolution of the electronic spectrum along the vertical dashed line in a). The red circle shows one Weyl point at the Fermi level (horizontal dashed line).

disorder, scattering, and interactions in the WSM makes modeling transport challenging.

A nice point of consistency of the proposed AIAO magnetic order is that it is characterized on Landau symmetry grounds by a simple Ising order parameter, for which a continuous thermal transition is allowed. As remarked earlier, the thermal MITs indeed appear continuous in the experiments. Adding finite temperature to the simple mean-field Hubbard model calculation further corroborates the expectation from Landau reasoning, showing that the magnetic transition is continuous, and its critical temperature grows with U, following the behavior of the charge excitation gap.[98] It may be interesting to study the corresponding thermal and quantum phase transitions in the future, for which the mean-field analysis may be inadequate.

4.   The role of many-body effects

In the preceding, we considered correlations only at the mean field level. This is expected on general grounds to be qualitatively correct for describing many phenomena within the phases so obtained. For example, in fully gapped states such as the TI or gapped AIAO phase, the gap cannot be broken by any small perturbation. The WSM is also stable to interactions, which are irrelevant

(marginally for long-range Coulomb) in the renormalization group sense, though they may have important transport consequences. A cellular dynamical mean field theory[104,105] (CDMFT) study bears out the robustness of the mean field treatment, though it shows that correlations may yet induce new phases: an axion insulator state appears in the CDMFT analysis[53,100] of Eq. (4) (plus Hubbard U) though it does not arise at the Hartree-Fock level. For these calculations, a convenient formulation of the $\mathbb{Z}_2$ topological invariant in terms of the *interacting* electron Green's function[67] was employed.

Other qualitative effects of correlations exist. Most obviously, it is likely that at least some of the quantum phase transitions indicated in Figure 5 are not fully captured by mean-field theory. Excitations and collective modes, which may be measured in the future by resonant inelastic x-ray scattering (RIXS) or other methods, typically mix elements of localized and itinerant systems in the intermediate correlation regime. Of course, neither CDMFT nor simpler Hartree-Fock theory are capable of capturing the more subtle quantum correlations in other proposed phases such as the topological Mott insulator, but we do not know that such phases can be found in the iridates.

5. Interactions with rare earth moments

We now briefly turn our attention to the interactions between the R-site f-electrons and the Ir d-electrons. Depending on the electronic configuration of the ion R^{3+}, the f-electrons can carry a net magnetic moment being in a Kramers doublet (R = Nd, Sm, Gd, Dy, Yb) or a non-Kramers one (Pr, Tb, Ho). Generally, if the Ir ions magnetically order, the rare earth spins must experience an exchange field, and also order at low temperature. Since $4f$ spins are rather highly localized, the exchange coupling between rare earth and Ir spins is expected, however, to be relatively weak, so the back-reaction on the Ir dynamics would be expected to be small. This is consistent with experiments[93] on Yb-227 and Y-227 which show spontaneous local fields in μSR at comparable temperatures (T_M = 130 K, 150 K, respectively), though Yb^{3+} carries a net moment while Y^{3+} does not. This is presumably Ir magnetism. Signs of Yb spin ordering or freezing appear only below $T^* \approx 20$ K.[93]

Nevertheless, the R spins can have a substantial influence on low energy properties, and their magnetism may be non-trivial. The most notable example is $Pr_2Ir_2O_7$, which remains metallic to low temperature, and shows no clear magnetic ordering transition.[106] Instead, novel freezing and non-Fermi liquid phenomena appear at low temperature, apparently driven by Pr magnetism.[106] Most strikingly, a zero field anomalous Hall effect has been observed below 1.5 K despite the absence of magnetic order or freezing for $T > 0.3$ K, leading to the proposal that this is a realization of a chiral spin liquid.[81,107] Spin-ice type physics for the Pr moments, *i.e.* predominantly 2-in/2-out configurations on each tetrahedron, has also been inferred. Several theoretical works[108–111] have suggested origins for these phenomena, including ordinary and exotic RKKY interactions, quadrupolar ordering, etc. As of this writing, the physics of $Pr_2Ir_2O_7$ remains unresolved. Overall, much less theoretical attention has been paid to the physics of other rare earths R, but one work

suggests their coupling to Ir may help to stabilize the WSM and axion insulator phases.[112]

6. Issues and Outlook

This section has outlined the theoretical and experimental work on the pyrochlore iridates. Both support a picture of the high-temperature state as a paramagnetic semi-metal, possibly a zero gap semiconductor. The MIT or crossover occurs simultaneously with the onset of commensurate magnetic order, most likely of AIAO type. While the transport phenomenology in these materials is very complex, and clearly requires more theoretical modeling, the rough behavior of the resistivity is in accord with static and dynamical mean-field-theory results: the on-set of the AIAO order would generally open up a charge gap in an otherwise metallic or semi-metallic paramagnetic state and the MIT temperature would become smaller as the relative correlation strength U/t gets weaker.[98] Understanding low temperature transport remains a challenge.

A direct determination of the magnetic structure of each member of the series is desirable, to confirm or disprove the AIAO for all or some compounds. It has been argued that the AIAO order observed at the Nd-sites in Nd-227 provides indirect evidence for the AIAO at the Ir sites, as the ordering at Nd sites may be caused by an effective field from the Ir's.[88] Recent resonant X-ray diffraction measurements on Eu-227[94] find $\boldsymbol{q} = 0$ magnetism with no indication of any lowering of lattice symmetry, prompting the authors of Ref. 94 to suggest that it must be the AIAO AF.

We have focused above primarily on possible electronic phases, but it is also important to understand various experimental observables. In particular, the excitation spectrum of the insulating and conducting states should be determined. An understanding of the effects of disorder and interactions on Weyl fermions is demanded to confront spectroscopic studies. As an example, the optical conductivities of Nd-227 and Rh-doped Nd-227 were recently measured.[113] The optical conductivity of Nd-227 has a striking charge gap while Rh-doped Nd-227 shows low-energy spectral weight that may be interpreted as an evidence for a WSM[113] (though in our opinion many other explanations are possible for the latter). There should also be collective magnetic excitations (magnons) and possibly excitons, which may be studied by resonant inelastic X-ray scattering (RIXS)[11–16] or other techniques. Theoretical calculations of both optics[98,100] and magnetic excitations[114] already exist for the phenomenological Hubbard model given in this review. Direct examination of surface states by photoemission or tunneling is challenging but of great interest.

III. STRONG MOTT REGIME

In this section, we consider "strong" Mott insulators, by which we mean materials for which it is sufficient to regard electrons as being localized effectively to single atoms, and a description in terms of local spin and orbital degrees of freedom applies. This requires *a priori* that the charge gap is large compared to the energy of spin and orbital excitations. In reality, spin-orbital exchange

Hamiltonians may also provide an intuitive description of some phenomena even in intermediate correlation situations, where charge fluctuations are significant. We will not comment further on this, and proceed with the strong Mott discussion.

The role of strong SOC in the strong Mott regime is clearly very different than that in more itinerant systems, since if electrons can be regarded as wholly localized, then considerations of *band* topology do not apply. In the strong Mott regime, instead, the interesting physics of SOC arises from the unique way in which it – wholly or partially – resolves *orbital degeneracy*. Orbital degeneracy is germane to correlated materials, in which the environment of transition metal atoms often has at least approximate octahedral or tetrahedral symmetry, resulting in degenerate doublets or triplets of orbitals. When these shells are neither half-filled nor full, orbital degeneracy arises. *In principle*, this leads, even without SOC, to interesting physics, in which the orbital degree of freedom behaves as an additional "pseudo-spin" quantum variable. The combined exchange of spin and pseudo-spin is given then by *Kugel-Khomskii models*.[115] In practice, the "quantumness" of the orbitals is usually compromised by the Jahn-Teller effect, in which lattice distortions spontaneously arise to split the orbital degeneracy.[116] Even at temperatures above this orbital ordering one, the associated phonon modes couple strongly to the orbital pseudo-spin, damping and decohering it. Consequently, a sadly mundane reduction of the beautiful Kugel-Khomskii Hamiltonian, by simply replacing the orbital pseudo-spin by its classical expectation value, seems to be adequate for the description of many orbitally degenerate transition metal systems, such as perovskite manganites. Even in the rare situations in which something more subtle is suspected, the mixing of orbital and lattice modes makes it practically difficult to clearly distinguish collective orbital excitations in experiments.

SOC offers a more interesting way of resolving orbital degeneracy, trading the Jahn-Teller effect for *entanglement* of spin and orbital degrees of freedom. It may entirely suppress the orbital degeneracy, leaving behind a pure Kramers doublet, as in the case of the $J_{\text{eff}} = 1/2$ states of Ir^{4+} ions, or even selecting a spin-orbital singlet state for some non-Kramers ions, as in the case of tetrahedral Fe^{2+}.[32] In other cases the degeneracy lifting may be partial, leading to effectively larger spin-orbital pseudo-spins. In either the Kramers or the latter case, the interactions amongst the remaining highly entangled states are strongly affected by this entanglement and the underlying spin-orbital exchange. Consequently, not only do such systems (at least largely) avoid the Jahn-Teller effect, but they enjoy exotic exchange interactions which foster unusual ground states. In the remainder of this section, we will discuss in particular the possibilities of *quantum spin liquid* and *multipolar ordered* phases, as well as unconventional magnetically ordered states. We illustrate these possibilities through two material examples, the honeycomb iridates and the double perovskites.

A.   Full degeneracy lifting and honeycomb iridates

As discussed already in Sec. II A 2, for an octahedrally coordinated Ir^{4+} ion with $5d^5$ config-uration, SOC completely removes orbital degeneracy, resulting in a maximally quantum effective spin-1/2 Hamiltonian, representing the $J_{\text{eff}} = 1/2$ states. One can say that the orbital degeneracy is fully lifted, the remaining degeneracy being guaranteed by Kramers theorem. The hexagonal iridates Na_2IrO_3 and Li_2IrO_3, which realize a layered structure consisting of a honeycomb lattice of Ir^{4+} ions, provide a concrete example of this case. Both compounds appear to be in the strong Mott regime. As shown by Jackeli and Khaliullin,[117] in the ideal limit, the edge sharing octahedral structure and the structure of the entangled $J_{\text{eff}} = 1/2$ orbitals leads to a cancellation of the usu-ally dominant antiferromagnetic oxygen-mediated exchange interactions. A sub-dominant term is generated by Hund's coupling, which takes the form of highly anisotropic exchange:

$$H_K = -K \sum_{\alpha=x,y,z} \sum_{\langle ij \rangle \in \alpha} S_i^\alpha S_j^\alpha \ , \tag{5}$$

where $\mathbf{S}_i$ are the effective spin-1/2 operators, and $\alpha = x, y, z$ labels both spin components and the three orientations of links on the honeycomb lattice. This peculiar and highly frustrated Hamiltonian is, remarkably, nearly the only example of an exactly soluble model for a quantum spin liquid state! As shown in an ingenious and tour de force paper by Alexei Kitaev,[118] it describes a state with no magnetic order and elementary excitations which are charge-neutral "spin"-carrying Majorana fermions that are their own anti-particles. It is astonishing that the Kitaev exchange form of Eq. (5), which is very unnatural for conventional magnetic systems, arises organically from the geometry and entanglement in the strong SOC limit.

The experimental situation is more complex. In this[119,120] and other[121] contexts, it has been argued that an isotropic Heisenberg interaction is generated from the direct overlap of $5d$ orbitals. The resulting Heisenberg-Kitaev model has been studied by several methods, which demonstrate that with increasing Heisenberg coupling the ground state undergoes successive transitions from the Kitaev spin liquid to a "stripy" four-sublattice magnetically ordered state, to the usual two sublattice one. Recent neutron scattering experiments and other studies show that the ground state of Na_2IrO_3 is, however, none of these states, but instead displays a different collinear mag-netic order, the so-called zig-zag state with a four-sublattice structure.[20,22] This has generated a number of new theoretical proposals to explain the apparent departure from the Heisenberg-Kitaev model.[122–126] Possibly important ingredients are other symmetry-allowed interactions on nearest-neighbor bonds, which might emerge from trigonal crystal fields or other mechanisms, and exchange with second and third neighbor sites. However, it has been suggested that the Kitaev interaction might be much larger in Li_2IrO_3 and the system may be closer to the quantum spin liquid phase.[18] It is perhaps worthwhile to comment on the role of frustration. Often in anti-ferromagnets, SOC, for example via the Dzyaloshinskii-Moriya interaction, is thought to remove accidental degeneracy and favor order. The Kitaev model is a counterexample, showing that in

some cases strong SOC can suppress ordering. However, one should be aware of both possibilities.

B. Partial degeneracy lifting and ordered double perovskites

In other situations, SOC may reduce but not eliminate fully the orbital degeneracy. Such partial degeneracy removal still has dramatic effects upon the physics. As an example, we consider a family of compounds with one or two electrons in the $4d$ or $5d$ shell. These are thus moderate to strongly spin-orbit coupled analogs of the very well studied $3d$ titanates with Ti^{3+} and vanadates with V^{3+} or V^{4+} states. The latter materials constitute classic families undergoing Mott transitions.[1] In octahedral coordination and for vanishing SOC, these valence states possess a three-fold orbital degeneracy, and consequently are Jahn-Teller active in the solid and tend to exhibit complex orbitally ordered states.

When SOC is dominant, we can understand the partial degeneracy lifting as follows. The t_{2g} orbitals split just as in iridates, but with the 1 or 2 electrons occupying now the $J_{\text{eff}} = 3/2$ quadruplet. In the d^1 case, this simply results in a $J_{\text{eff}} = 3/2$ local effective spin. In the case of the d^2 electron configuration, the description based purely on single-particle states no longer holds, but the result is similar. Following Hund's rules applied to the d^2 configuration, one finds a total spin $S = 1$ and an effective orbital angular momentum (three-fold degeneracy) $L_{\text{eff}} = 1$. In the end S and L align, so that an effective $J_{\text{eff}} = 2$ spin results when SOC is included.[57,127] We see that in both cases, the ionic degeneracy ($= 4, 5$ for d^1 and d^2, respectively) is reduced from that without SOC ($= 6, 9$, respectively), but is still larger than what is required by Kramers theorem alone ($= 2, 1$).

What physics can we expect from the effective spins? "Large" spins such as $S = 3/2, 2$ are often thought to behave relatively classically. This is based on the standard spin wave expansion for Heisenberg-type models, which indeed can be cast as an expansion in $1/S$. However, the classicality of such spins in fact depends critically on the nature of their interactions. Many examples of non-classical behavior for larger spins can be found in the theoretical literature, notably spin-nematic or quadrupolar ordered phases of spin one systems with biquadratic exchange,[128] Haldane type states for $S \geq 1$ AKLT models,[129] and quantum spin liquid states of large N SU(N) and Sp(N) antiferromagnets.[130] All these cases can be cast in the form of models in which spins with $S > 1/2$ interact with *higher order exchange* interactions involving multiple spin operators on each site (but typically with spins still interacting pairwise). One can describe such interactions as consisting of coupling between *multipole* moments (beyond dipoles) of the spins. Heuristically, multipolar interactions enhance quantum fluctuations because they connect directly states with very different S^z quantum numbers, allowing the wavefunction to easily delocalize in the spin space. By contrast, the usual bilinear Heisenberg interactions induce only single spin flips, and consequently tend to localize the spin wavefunction near some classical extremum.

Unfortunately, multipolar interactions are very weak in conventional systems with weak SOC. However, this is not true for the effective spins in the strong SOC limit. This is because spin

exchange is *always* dependent on the orbital state, and in the strong SOC limit spins and orbitals are highly entangled. This entanglement transfers the orbital dependence of the exchange to the effective spin, generating multipolar exchange, as explained in Sec. III B 2. Thus for spin-orbitally entangled effective spins, *strong multipolar exchange is generic*. We illustrate this in the following subsections for one class of materials.

1. Double perovskites

For numerous examples of partially quenched degeneracy of the above type, we turn to the double perovskite materials, $A_2BB'O_6$, whose structure is shown in Figure 6(a). It can be derived from the simpler cubic perovskite structure, ABO_3, but replacing the single B atom by alternating B and B' atoms on two rock-salt sublattices. There are many such compounds with non-magnetic B sites and B' sites occupied by the $4d$ and/or $5d$ transition metal elements with d^1 or d^2 config-uration. Because of the difference in the valence charges and ionic radius between B and B' ions, the magnetic B' ions form an fcc lattice structure with very little intersite disorder, and the lattice constant twice that of the original cubic case. As shown in Table II, the magnetic ions B' (Re^{6+}, Os^{7+}, Mo^{5+} for d^1 or Re^{5+}, Os^{6+} for d^2) have one or two electrons on the $4d$ or $5d$ shell.[34–47] Like Iridium, such heavy elements and high orbital shells naturally incorporate strong SOC. Moreover, the large separation of the metal ions in this structure suppresses electron hopping and promotes Mott insulating behavior.

Immediate evidence for orbital degeneracy lifting can be found in several of these materials. One consequence of the strong SOC limit is a reduction of the effective moment. For the $J_{eff} = 3/2$ state, in fact, in an ideal isolated ion, the orbital and spin contributions cancel, and the moment *vanishes*, *i.e.* the g-factor is zero! Due to mixing with neighboring oxygen ions, the magnetic moment is generally non-zero in the solid, but a small g-factor is still expected. The situation for $J_{eff} = 2$ is similar, but less dramatic: the magnetic moment is reduced to $\boldsymbol{M} = \boldsymbol{S}_{eff}/2$, *i.e.* $g = 1/2$. Indeed, the magnetic moments of most compounds in Table II are smaller than the values expected from a spin-only contribution, consistent with the effective local moment renormalized by the strong SOC.[56,57,131,132]

Another indicator of strong SOC is the magnetic entropy, which can give direct evidence of the quadruplet or quintuplet structure. In Ba_2YMoO_6, an entropy of $R\ln 4$ (here R is the gas constant) was indeed estimated from integration of the magnetic specific heat,[35] consistent with the $J_{eff} = 3/2$ state.

2. Multipolar exchange

We now explain how multipolar exchange arises from spin-orbital entanglement, a known phe-nomena in f-electron systems.[3] The basic idea is to consider the Kugel-Khomskii type exchange

that arises when all orbitals are included, and then to *project* that exchange to the effective spins that form in the strong SOC limit. In general, several different exchange processes contribute to the appropriate Kugel-Khomskii model for double perovskites. For simplicity, we will just illustrate one in detail here, and refer the reader to Refs. 56 and 57 for more details. We consider the d^1 case, and focus on the nominally antiferromagnetic nearest-neighbor process via intermediate oxygens, which would be expected to dominate. These processes are strongly restricted by orbital degrees of freedom. As is illustrated in Figure 6(b), in xy planes, only electrons residing on d_{xy} orbitals can virtually transfer to neighboring sites via p_x and p_y orbitals of the intermediate oxygens (the same process may be understood as direct exchange between molecular orbitals consisting of transition metal d_{xy} and neighboring oxygen p levels). Therefore, the antiferromagnetic exchange interaction can be written as $\mathcal{H}_{\mathrm{ex}} = \mathcal{H}_{\mathrm{ex}}^{xy} + \mathcal{H}_{\mathrm{ex}}^{yz} + \mathcal{H}_{\mathrm{ex}}^{xz}$ with

$$\mathcal{H}_{\mathrm{ex}}^{xy} = J \sum_{\langle ij \rangle \in xy \text{ plane}} \left(\boldsymbol{S}_{i,xy} \cdot \boldsymbol{S}_{j,xy} - \frac{1}{4} n_{i,xy} n_{j,xy} \right), \tag{6}$$

where the sum is over nearest neighbor sites in the xy planes, and the corresponding terms in yz and xz planes are obtained by a cubic permutation. Here the operators $\boldsymbol{S}_{i,xy}$ and $n_{i,xy}$ denote the spin residing on the d_{xy} orbital and d_{xy}-orbital occupation number at site i, respectively.

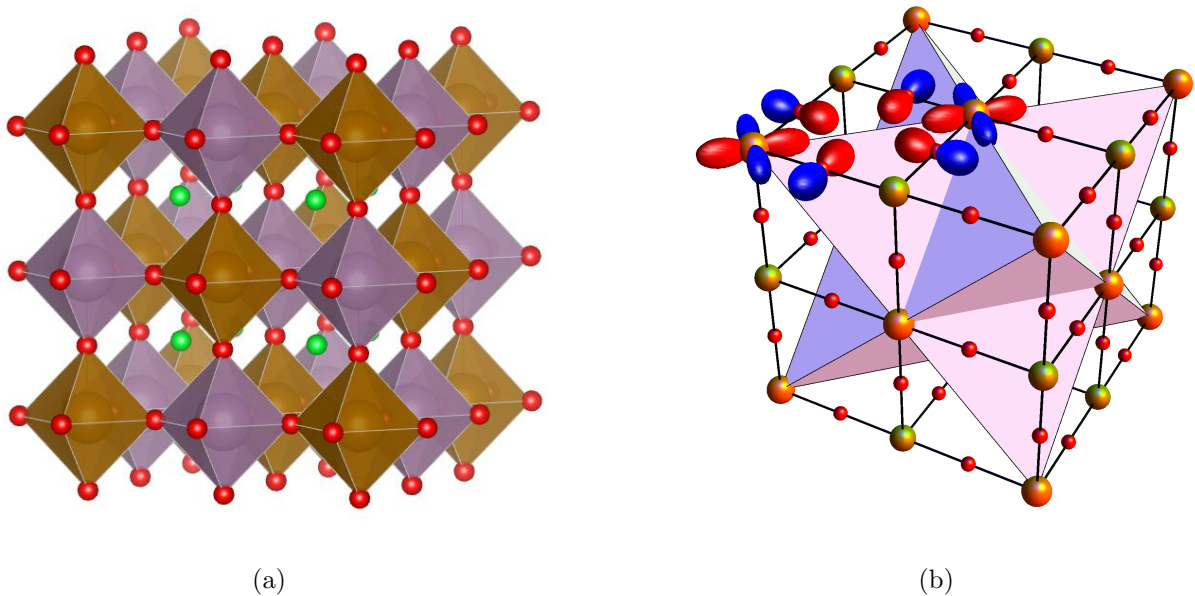(a)   (b)

FIG. 6. a) The crystal structure of ordered double perovskite, $A_2 B B' O_6$. The green spheres, purple octahedra, and dark yellow octahedra represent A-site ions, $B O_6$ octahedra, and $B' O_6$ octahedra, respectively. b) The same structure, showing the representation of the geometrically frustrated fcc lattice of B sites (orange spheres) as edge sharing tetrahedra. Two d_{xy} orbitals on nearest-neighbor B sites are shown with the intermediate p_x, p_y orbitals involved in their exchange path. In this picture B' sites are golden, and O sites are red, and A sites are not shown.

TABLE II. A list of representative ordered double perovskites in which the magnetic ions have d^1 or d^2 electron configuration. Variations in the Curie-Weiss temperature Θ_{CW} and effective magnetic moment μ_{eff} may originate from the experimental fitting of data at different temperature ranges. In the Table, PM = paramagnetic, AFM = antiferromagnetic, and FM = ferromagnetic phase. T_c is the ordering temperature, and T_G is the glass transition temperature.

Compound	B'	electron config.	Θ_{CW} (K)	μ_{eff} (μ_B)	magnetic transition	Refs
Ba_2YMoO_6	Mo^{5+}	$4d^1$	$-91 \sim -219$	$1.34 \sim 1.72$	PM down to 2K	34–39
Sr_2MgReO_6	Re^{6+}	$5d^1$	-426	1.72	spin glass, $T_G \sim 50K$	41
Ba_2NaOsO_6	Os^{7+}	$5d^1$	~ -10	~ 0.6	FM $T_c = 6.8K$	45
Ba_2CaOsO_6	Os^{6+}	$5d^2$	-157	1.61	AF $T_c = 51K$	43
La_2LiReO_6	Re^{5+}	$5d^2$	-204	1.97	PM down to 2K	40

Without SOC, and as written, the above interaction appears relatively conventional and in particular is bilinear in $\boldsymbol{S}_{i,xy}$. However, this can be rewritten by explicitly representing the orbital degree of freedom via the effective $L = 1$ angular momentum $\boldsymbol{L}$ describing the t_{2g} degree of freedom. One has $\boldsymbol{S}_{i,xy} = \boldsymbol{S}_i^{\text{tot}}[1 - (L_i^z)^2]$ and $n_{i,xy} = 1 - (L_i^z)^2$, where $\boldsymbol{S}_i^{\text{tot}} = \boldsymbol{S}_{i,xy} + \boldsymbol{S}_{i,xz} + \boldsymbol{S}_{i,yz}$ is the total true spin on site i. With these substitutions, we see that up to 3 spin or pseudo-spin operators are multiplied on each site i or j. Now in the strong SOC limit, *i.e.* $J \ll \lambda$, this should be projected onto the $J_{\text{eff}} = 3/2$ effective spin. That is, we should replace $\mathcal{H} \to \tilde{\mathcal{H}}$, in which operators on each site have been replaced by their projections, $\tilde{\mathcal{O}} = \mathcal{P}_{\frac{3}{2}}\mathcal{O}\mathcal{P}_{\frac{3}{2}}$, where $\mathcal{P}_{\frac{3}{2}}$ is the projection operator onto the $J_{\text{eff}} = 3/2$ multiplet. Some algebra shows that these projections are quite non-trivial:

$$\tilde{S}_{i,xy}^\alpha = \frac{1 + 2\delta_{\alpha,z}}{4}S_i^\alpha - \frac{1}{3}S_i^z S_i^\alpha S_i^z \quad (\alpha = x, y, z), \qquad \tilde{n}_{i,xy} = \frac{3}{4} - \frac{1}{3}(S_i^z)^2, \tag{7}$$

where $\boldsymbol{S}_i$ is the final projected $J_{\text{eff}} = 3/2$ effective spin. Spin and occupation number operators for other orbitals can be readily generated by a cubic permutation.

The quadratic and cubic products of S_i^μ represent components of the quadrupolar and octupolar tensors, respectively. We see that the innocuous-looking Hamiltonian in Eq. (6) is transformed, after the strong SOC projection using $\mathcal{O} \to \tilde{\mathcal{O}}$ via Eq. (7), into a highly non-trivial interaction with octupolar and quadrupolar couplings of the same order as ordinary bilinear exchange. This mechanism generating higher-order spin exchange is quite generic, and applies equally to all the
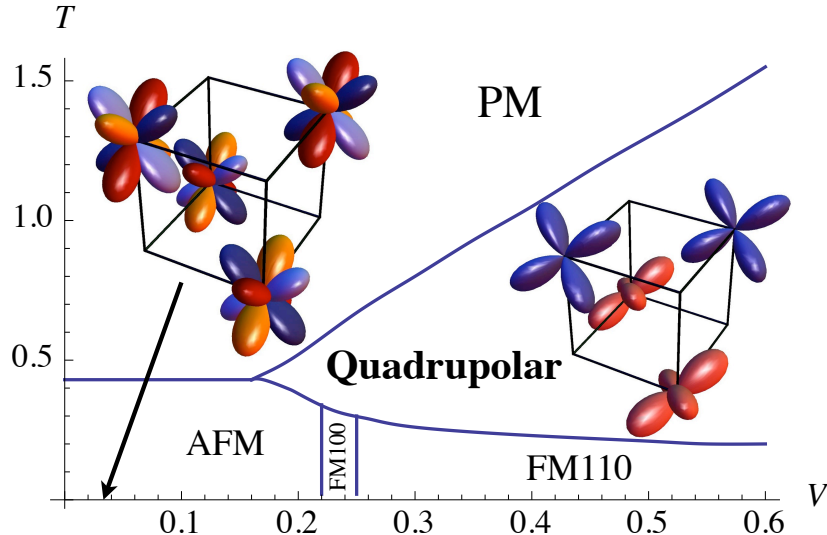
FIG. 7. A cut of the mean field phase diagram for d^1 double perovskites at fixed $J' = 0.2J$, and $J = 1$, as a function of temperature T and electric quadrupole interaction V. The antiferromagnetic (AFM) state is illustrated at $T = 0$ by an image of the orbital wavefunctions for $S^x = +1/2$ (with positive/negative regions colored blue/light blue) and for the $S^x = -1/2$ (with positive/negative regions colored red/orange). In the quadrupolar state, the charge density is shown. The FM110 and FM100 are ferromagnetic states with net magnetization along the [110] and [100] axes (and spin-orbital entanglement which is difficult to illustrate). The curves are obtained from calculations in Ref. 56.

interactions in a typical strong SOC situation. It gives access to a variety of exotic physics of multipolar systems.[133,134]

For the d^1 double perovskites, two natural additional exchange channels were identified between nearest-neighbors in Ref. 56: a ferromagnetic exchange J' between orthogonal orbitals, and an electrostatic quadrupole interaction V. Details of these interactions can be found in Ref. 56. Similar considerations apply to the d^2 case, as described in Ref. 57. All the interactions in both cases become multipolar in character after the strong SOC projection.

3. Mean field theory

With the exotic interaction Hamiltonians discussed above, unusual phases are expected even in a mean field treatment. We explore this here, and subsequently consider the possibility of phases beyond mean field theory. The Weiss mean field treatment consists, as usual of decoupling the interactions between sites, to generate self-consistent single site problems. Due to the multipolar interactions, each single site Hamiltonian contains not only an effective Zeeman field, but also effective quadrupolar and octupolar anisotropies. The latter define additional multipolar order parameters in the mean field theory. A full analysis is given in Ref. 56 for the d^1 case and Ref. 57 for the d^2 case. We summarize only the former as an example.

A representative cut through the three-dimensional phase diagram is depicted in Figure 7. At zero temperature three phases appear, all with nominally "conventional" ferromagnetic or antiferromagnet dipolar magnetic order. However, there are unconventional aspects revealed upon closer inspection.

The simplest state is the antiferromagnetic phase, appearing for small J'/J and V/J. It has a conventional two-sublattice structure, with states on either sublattice related by time reversal. However, although it displays local static dipole moments, their magnitude is small, and in fact *vanishes* as temperature $T \to 0$. This is particularly surprising in a mean field theory (for a conventional Heisenberg system mean field theory gives a full moment). In fact, accompanying the dipole moment is a large *staggered octupole moment*, which competes with and suppresses substantially the dipolar order.

With larger J'/J and V/J, the system develops ferromagnetic phases, FM110 and FM100 with net ferromagnetic moments along [110] and [100] directions, respectively. These two non-uniform ferromagnets are rather unconventional as they actually have a two sublattice structure, with partial cancellation of non-parallel magnetic moments in the ferromagnetic magnetization. In fact, the two sublattice structure is a manifestation of staggered quadrupolar order, and it is this quadrupolar ordering which predominantly drives the formation of these two phases. The magnetism develops atop it. Since orbital polarization is distinct on the two sublattices, they cannot be time-reversal conjugates, and consequently when magnetism onsets, a net ferromagnetic moment results.

The driving role of the quadrupolar order can be seen from the $T > 0$ phase diagram. Over a wide range of intermediate temperature, the ferromagnetic order is destroyed, the FM region (and part of the AFM one) being replaced by a purely quadrupolar ordered phase. In the quadrupolar phase, time-reversal symmetry is unbroken, which is sufficient to require the dipolar and octupolar order parameters to vanish. A standard classification scheme for quadrupolar states is to examine the eigenvalues of the traceless quadrupolar tensor $Q_i^{\mu\nu} = \langle S_i^\mu S_i^\nu \rangle - \frac{1}{3}S(S+1)\delta^{\mu\nu}$, where the eigenvalues must sum to zero (here $S = 3/2$ for d^1). The quadrupolar phase with only one independent eigenvalue, *i.e.* eigenvalues$(Q) = \{q, q, -2q\}$, is called the *uniaxial nematic phase*, and corresponds to the situation, where one principal axis is distinguished from the other two that remain equivalent. This type of "spin nematic" has been studied theoretically in $S = 1$ Heisenberg models with strong biquadratic interactions,[128] though it is hard to achieve such strong biquadratic exchange in conventional systems. In the most general case, there may be two independent eigenvalues, *i.e.* eigenvalues$(Q) = \{q_1, q_2, -q_1 - q_2\}$, with $q_1 \neq q_2$. This is called a *biaxial nematic phase*, where all three principal axes are non-equivalent. The quadrupolar state obtained here is such a biaxial nematic phase.

Such a quadrupolar phase also exists in the phase diagram for the d^2 double perovskites,[57] but in that case appears even at $T = 0$. This difference between the d^1 and d^2 cases occurs because within Weiss mean field theory, a Kramers ion such as d^1 must always break time reversal symmetry at $T = 0$ to avoid ground state degeneracy.

4. Beyond mean-field theory

As remarked earlier, multipolar interactions tend to destabilize conventional, magnetically ordered semiclassical ground states. Roughly speaking, this is because they contain many more "spin flip" terms analogous to the $S_i^+ S_j^-$ couplings which are part of the usual Heisenberg two spin interactions. Quantum disordered ground states can be established rigorously for AKLT models,[129] which have specially tuned SU(2) invariant Hamiltonians which can be written entirely in terms of a positive semi-definite sum of projection operators. They can also be found in a controlled manner for large N models with enlarged SU(N) or Sp(N) symmetry.[130] Neither approach can be directly applied here, but it is clear that the multipolar Hamiltonians which occur naturally for d^1 and d^2 systems are somewhat intermediate between conventional spin models and these special cases. Thus in frustrated geometries, quantum disordered states may well obtain.

A simple way to check for disordered states is to gauge the magnitude of quantum fluctuations within a spin-wave expansion (generalized for multipolar phases) about the mean field states. Indeed using a generalized Holstein-Primakoff spin wave theory, it is shown that quantum fluctuations are strong when J'/J and V/J are small.[56] This strongly points to effects beyond mean field, and the likelihood of a non-magnetic ground state. By examining various limits, both valence bond solid and quantum spin liquid states were proposed for this region of the phase diagram of the d^1 systems in Ref. 56. Further quantitative study of models of this type would be highly desirable, but this is challenging and probably requires at least significant extension of existing numerical methods.

Other theoretical work has considered the effects of non-cubic crystal fields, which split the quadruplet ground state to form a low energy doublet. This then reduces to an effective $S = 1/2$ model, but with highly anisotropic interactions with anisotropy depending on the bond orientation. The resulting exchange model may be strongly frustrated. In such cases, quantum fluctuations may also support a quantum spin liquid phase,[58] which is amenable to analysis by more conventional methods.

5. Connections to experiments

A detailed discussion about the applications of theory to experiment, and on specific materials, can be found in Ref. 56 and Ref. 57. Here we comment just on a few examples for which strong SOC phenomenology is most compelling. In general, for the strong SOC limit to apply, both non-cubic crystal fields and exchange interactions should be small compared to the spin orbit splitting. The latter is of order 100 meV for $4d$ materials like Mo^{5+}, and a few times larger for the $5d$ materials. This is quite large compared to exchange interactions in double perovskites, but not necessarily large compared to crystal field perturbations in non-cubic crystals. Thus we focus on cases where at least elastic X-ray scattering measurements find a cubic structure. This presumably indicates the absence of a static Jahn-Teller effect, though the dynamic or non-uniform effects of Jahn-Teller

phonon coupling may still be important.

We have already mentioned Ba_2YMoO_6, which remains cubic to low temperatures and has a magnetic entropy approximately equal to $R \ln 4$, consistent with a $J_{eff} = 3/2$ local moment.[35] This material avoids any apparent phase transitions down to 2 K, despite rather strong antiferromagnetic interactions. An energy gap is indicated in recent NMR and inelastic neutron scattering measurements, which may be associated with valence bond formation.[37] An unusual feature seen in this material, which occurs in a number of double perovskites, is the existence of *two* Curie regimes in the magnetic susceptibility: above 100 K and below 50 K.[35,36,38] This is suggestive of some single-ion anisotropy, which would explain the existence of two Curie regimes because it splits the 4-fold degeneracy of the $J_{eff} = 3/2$ states but leaves a 2-fold Kramers doublet at temperatures below 50 K, which still gives a Curie signal. This could perhaps be associated with quadrupolar order, or to a lattice driven distortion. The macroscopic cubic symmetry appears at odds with the latter, but a set of random local distortions with statistical cubic symmetry might be a possibility. More recent experiments have observed the emergence of additional phonon mode below 130 K, consistent with a local structural change.[38]

A second example is Ba_2NaOsO_6, for which the ground state below 6.8 K was found to be ferromagnetic with easy axis along the [110] direction.[45] The [110] easy axis is quite unusual, and indeed does not occur in standard Landau theory for ferromagnets, in which weak cubic anisotropy (quartic terms) always selects either a [100] or [111] axis. This is a strong indication for some correct element in the strong SOC description, which indeed predicts [110] ferromagnetism to be dominant, due to the quadrupolar mechanism. Experimental confirmation would require measurement of a structure change associated to the quadrupolar ordering, which so far has not been observed. However, several other indications are in favor of quadrupolar ordering.[56]

IV. CONCLUDING REMARKS AND OUTLOOK

The investigation of correlated electron systems with strong spin-orbit coupling (SOC) is still in its infancy. In this review, we summarized and explained recent developments in theoretical and experimental research in this rapidly growing area. We show that SOC tends to act with Coulomb interactions to enhance the degree of electron correlations, producing spin-orbit-assisted Mott insulators. In the weak to intermediate correlation regime, we described possible electronic states with topological band structures. When correlations are strong enough that a local moment description applies, we discussed how spin liquid and multipolar phases may occur due to spin-orbital entanglement. We explored possible applications to pyrochlore iridates in the weak-to-intermediate correlation regime, and honeycomb iridates and double-perovskites with $4d/5d$ transition metal elements in the strong Mott regime.

Due to space limitations, many important systems were not discussed. This includes the Ruddlesdon-Popper series of perovskite iridates,[9–16,135–137] $Sr_{n+1}Ir_nO_{3n+1}$, whose $n = \infty, 1, 2$ members are some of the most investigated materials in this class. In particular, Sr_2IrO_4 warrants spe-

cial attention as an approximate homolog of the parent material of some of the high-T_c cuprates, La_2CuO_4. Like the latter, Sr_2IrO_4 is an antiferromagnetic insulator,[9–13] with a very large exchange constant $J \sim 700 - 1000$ K,[11–13] somewhat smaller than but comparable to that of the cuprates, and a charge gap $\Delta_c \sim 350 - 650$ meV or $4000 - 7500$ K, many times larger than J. Both Sr_2IrO_4 and $Sr_3Ir_2O_7$ have served as striking examples of the power of modern RIXS, which is remarkably suited for $5d$ compounds.[10–16] RIXS has provided a direct probe of spin and orbital states and dynamics. By RIXS, it has been possible to test and confirm the $J_{eff} = 1/2$ character of the Ir^{4+} state in Sr_2IrO_4[10] and to measure the full spin-wave dispersion in both compounds.[11–16] Such measurements reinforce the analogy of Sr_2IrO_4 to the cuprates, and have motivated a strong push to *dope* this material[138–140] in hopes of finding high-temperature superconductivity, pseudo-gap behavior, etc, as also suggested theoretically.[141] This program is very much underway, though at the time of this writing superconductivity has not been found.

In general, doping of correlated insulators with strong SOC is a very interesting subject. In the traditional venue, the Mott metal-insulator *quantum* phase transition may be tuned either by bandwidth control at fixed stoichiometric filling, or by filling control, varying the carrier density, and these two types of Mott transitions have quite distinct characters.[2] In this Review we have already remarked upon the seemingly distinct behavior of the bandwidth controlled transition (and the thermal transition at fixed filling) in the strong SOC regime from the usual strong first order one in $3d$ transition metal compounds. It may be that the filling controlled transitions are also qualitatively different in the strong SOC case. There is very little theoretical work on this problem,[141–143] which promises to be a rich subject for future study, and not only in Sr_2IrO_4.

Another important topic which has been mentioned but not given in depth attention in this review is the emergence of fractionalized exotic phases from topological bands. This possibility is vetted experimentally and theoretically by the most studied fractionalized states of matter, the Fractional Quantum Hall Effect (FQHE) state of two-dimensional electron gases in high magnetic fields. The Landau levels of that problem can be view as the simplest examples of bands with non-trivial Chern number, and it is understood that the FQHE originates from interacting electrons that partial fill a Landau level. Many theorists have suggested that FQHE may occur due to fractionally filled bands with non-trivial Chern number in crystalline materials with broken time-reversal symmetry: a fractional Chern insulator.[77–79] Time-reversal symmetric fractional topological insulators[144–146] have also been proposed in both 2D and 3D, as have other fractionalized phases such as the topological Mott insulator.[8,55] While current theoretical understanding demonstrates clearly that all these phases *may* exist, *i.e.* that they are stable phases of matter for some Hamiltonian parameters, they are all outside the domain of conventional mean field approaches, including those combined with *ab initio* methods such as LDA+U and DMFT. For many of the other phases described in this review, however, mean field approaches are adequate.

Also beyond these mean field approaches are numerous possible quantum critical points (as well as thermal ones). The rich variety of phases found already in the studies discussed in this review implies that suitable phase transitions between these phases should be accessible. This includes

of course MITs, but also transitions to the onset of magnetic order, and between different types of band topology. In many experimental systems with weak SOC, quantum criticality is seen to coincide with unconventional superconductivity, and many believe the former is a causative factor in the latter.[147] It will be very interesting to seek superconductivity from quantum critical fluctuations in strong SOC materials, and if it exists, to see whether topological superconductivity might result. Experimentally, strong SOC tightens the link between electronic and lattice structure, so that a very strong influence of pressure/strain may be expected in these materials. We anticipate a growing number of studies of criticality in this class of systems.

As in any developing field, there are controversies. The $J_{\text{eff}} = 1/2$ limit is actively debated in different iridates. The degree of spin-orbital entanglement can be addressed by several distinct experiments, and should vary from material to material, depending upon the strength of crystal fields, etc. While the $J_{\text{eff}} = 1/2$ picture is appealing and simple, it is probably, however, not essential to many of the phenomena we have discussed. Also at issue is the nature of the correlated insulating state. Some authors distinguish "Mott" and "Slater" insulators, where in the latter case insulating behavior is due to magnetic order. It is not clear whether this distinction is well-defined, especially at zero temperature, given that magnetic order itself can arise only from Coulomb interactions. In general, there is no reason to have a phase transition as the interaction strength is increased up to the local moment regime, if the magnetic ordering pattern is unchanged. Different experiments[148,149] that try to differentiate the two may be formulated: is the system conducting or insulating above the magnetically ordering temperature? Is the charge gap Δ_c large compared to the exchange J? Is the MIT continuous or first order? These criteria need not agree. A related issue is the "degree of correlation" in, $e.g.$ iridates, with presumably Slater insulators being less correlated. This question is typically posed by $ab\ initio$ based approaches such as LDA+U or DMFT. We remark that by these techniques, even the correlation strength of high-T_c cuprates might be questioned,[150] so the physical significance of this question is opaque to us. Finally, the strong SOC limit itself is open to question. The strong SOC limit indeed depends not only upon the ratio of SOC to non-cubic crystal fields, but also on the strength of hopping or exchange relative to SOC. Mazin $et\ al.$ have suggested indeed that SOC is not critical to the insulating state in Na_2IrO_3.[151,152]

Moving beyond these debates, perhaps one of the most ambitious programs for the future is "engineering" desired electronic states. An appealing possibility is combining the materials discussed in this review with advances in layer by layer atomic growth of oxides to produce designer heterostructures of iridates and other strong SOC systems. For example, various heterostructures of perovskites,[153,154] (including $SrIrO_3$) as well as of $R_2Ir_2O_7$ along the [111] direction[155] have been proposed and several non-trivial phases such as topological insulators and quantum Hall states are predicted to exist under certain conditions. Experiments of this type are within the realm of possibility in the near future.

At the time of writing, the materials synthesis and experimental characterization of diverse $4d$ and $5d$ transition metal oxides is only increasing. The effects of carrier doping, hydrostatic

pressure, and high magnetic fields are under investigation. The outcome of these experiments and existing and future theory may uncover entirely new classes of many-body quantum ground states in strongly spin-orbit coupled systems.

ACKNOWLEDGMENTS

[1] N. F. Mott, *Metal-insulator transitions* (Taylor & Francis London, 1990).

[2] M. Imada, A. Fujimori, and Y. Tokura, Rev. Mod. Phys. **70**, 1039 (1998).

[3] P. Santini, S. Carretta, G. Amoretti, R. Caciuffo, N. Magnani, and G. H. Lander, Rev. Mod. Phys. **81**, 807 (2009).

[4] M. Z. Hasan and C. L. Kane, Rev. Mod. Phys. **82**, 3045 (2010).

[5] X.-L. Qi and S.-C. Zhang, Reviews of Modern Physics **83**, 1057 (2011).

[6] M. Z. Hasan and J. E. Moore, Annual Review of Condensed Matter Physics **2**, 55 (2011).

[7] A. Georges, L. de Medici, and J. Mravlje, Annual Review of Condensed Matter Physics **4**, 137 (2013), arXiv:1207.3033 [cond-mat.str-el].

[8] D. Pesin and L. Balents, Nature Physics **6**, 376 (2010).

[9] B. J. Kim, H. Jin, S. J. Moon, J.-Y. Kim, B.-G. Park, C. S. Leem, J. Yu, T. W. Noh, C. Kim, S.-J. Oh, J.-H. Park, V. Durairaj, G. Cao, and E. Rotenberg, Phys. Rev. Lett. **101**, 076402 (2008).

[10] B. J. Kim, H. Ohsumi, T. Komesu, S. Sakai, T. Morita, H. Takagi, and T. Arima, Science **323**, 1329 (2009).

[11] S. Fujiyama, H. Ohsumi, T. Komesu, J. Matsuno, B. J. Kim, M. Takata, T. Arima, and H. Takagi, Phys. Rev. Lett. **108**, 247212 (2012).

[12] J. Kim, D. Casa, M. H. Upton, T. Gog, Y.-J. Kim, J. F. Mitchell, M. van Veenendaal, M. Daghofer, J. van den Brink, G. Khaliullin, and B. J. Kim, Phys. Rev. Lett. **108**, 177003 (2012).

[13] J. W. Kim, Y. Choi, J. Kim, J. F. Mitchell, G. Jackeli, M. Daghofer, J. van den Brink, G. Khaliullin, and B. J. Kim, Phys. Rev. Lett. **109**, 037204 (2012).

[14] J. Kim, A. H. Said, D. Casa, M. H. Upton, T. Gog, M. Daghofer, G. Jackeli, J. van den Brink, G. Khaliullin, and B. J. Kim, Phys. Rev. Lett. **109**, 157402 (2012).

[15] S. Fujiyama, K. Ohashi, H. Ohsumi, K. Sugimoto, T. Takayama, T. Komesu, M. Takata, T. Arima, and H. Takagi, Phys. Rev. B **86**, 174414 (2012).

[16] P. D. C. King, T. Takayama, A. Tamai, E. Rozbicki, S. M. Walker, M. Shi, L. Patthey, R. G. Moore, D. Lu, K. M. Shen, H. Takagi, and F. Baumberger, Phys. Rev. B **87**, 241106 (2013), arXiv:1302.0433 [cond-mat.str-el].

[17] Y. Singh and P. Gegenwart, Phys. Rev. B **82**, 064412 (2010).

[18] Y. Singh, S. Manni, J. Reuther, T. Berlijn, R. Thomale, W. Ku, S. Trebst, and P. Gegenwart, Phys. Rev. Lett. **108**, 127203 (2012).

[19] H. Gretarsson, J. P. Clancy, X. Liu, J. P. Hill, E. Bozin, Y. Singh, S. Manni, P. Gegenwart, J. Kim, A. H. Said, D. Casa, T. Gog, M. H. Upton, H.-S. Kim, J. Yu, V. M. Katukuri, L. Hozoi, J. van den Brink, and Y.-J. Kim, Phys. Rev. Lett. **110**, 076402 (2013).

[20] X. Liu, T. Berlijn, W.-G. Yin, W. Ku, A. Tsvelik, Y.-J. Kim, H. Gretarsson, Y. Singh, P. Gegenwart, and J. P. Hill, Phys. Rev. B **83**, 220403 (2011).

[21] J. P. Clancy, N. Chen, C. Y. Kim, W. F. Chen, K. W. Plumb, B. C. Jeon, T. W. Noh, and Y.-J. Kim, Phys. Rev. B **86**, 195131 (2012).

[22] S. K. Choi, R. Coldea, A. N. Kolmogorov, T. Lancaster, I. I. Mazin, S. J. Blundell, P. G. Radaelli, Y. Singh, P. Gegenwart, K. R. Choi, S.-W. Cheong, P. J. Baker, C. Stock, and J. Taylor, Phys. Rev. Lett. **108**, 127204 (2012).

[23] D. Yanagishima and Y. Maeno, Journal of the Physical Society of Japan **70**, 2880 (2001).

[24] K. Matsuhira, M. Wakeshima, R. Nakanishi, T. Yamada, A. Nakamura, W. Kawano, S. Takagi, and Y. Hinatsu, Journal of the Physical Society of Japan **76**, 043706+ (2007).

[25] T. F. Qi, O. B. Korneta, X. Wan, L. E. DeLong, P. Schlottmann, and G. Cao, Journal of Physics: Condensed Matter **24**, 345601 (2012).

[26] Y. Okamoto, M. Nohara, H. Aruga-Katori, and H. Takagi, Phys. Rev. Lett. **99**, 137207 (2007).

[27] H. Kuriyama, J. Matsuno, S. Niitaka, M. Uchida, D. Hashizume, A. Nakao, K. Sugimoto, H. Ohsumi, M. Takata, and H. Takagi, Applied Physics Letters **96**, 182103 (2010).

[28] Y. G. Shi, Y. F. Guo, S. Yu, M. Arai, A. A. Belik, A. Sato, K. Yamaura, E. Takayama-Muromachi, H. F. Tian, H. X. Yang, J. Q. Li, T. Varga, J. F. Mitchell, and S. Okamoto, Phys. Rev. B **80**, 161104 (2009).

[29] J. Yamaura, K. Ohgushi, H. Ohsumi, T. Hasegawa, I. Yamauchi, K. Sugimoto, S. Takeshita, A. Tokuda, M. Takata, M. Udagawa, M. Takigawa, H. Harima, T. Arima, and Z. Hiroi, Phys.

Rev. Lett. **108**, 247205 (2012).

[30] A. Krimmel, M. Mücksch, V. Tsurkan, M. M. Koza, H. Mutka, and A. Loidl, Phys. Rev. Lett. **94**, 237402 (2005).

[31] N. Büttgen, A. Zymara, C. Kegler, V. Tsurkan, and A. Loidl, Phys. Rev. B **73**, 132409 (2006).

[32] G. Chen, L. Balents, and A. P. Schnyder, Physical Review Letters **102**, 096406 (2009).

[33] G. Jackeli and G. Khaliullin, Physical Review Letters **103**, 067205 (2009), arXiv:0906.2733 [cond-mat.str-el].

[34] E. J. Cussen, D. R. Lynham, and J. Rogers, Chem. Mater. **18**, 2855 (2006).

[35] M. A. de Vries, A. C. Mclaughlin, and J.-W. G. Bos, Phys. Rev. Lett. **104**, 177202 (2010).

[36] T. Aharen, J. E. Greedan, C. A. Bridges, A. A. Aczel, J. Rodriguez, G. MacDougall, G. M. Luke, T. Imai, V. K. Michaelis, S. Kroeker, H. Zhou, C. R. Wiebe, and L. M. D. Cranswick, Phys. Rev. B **81**, 224409 (2010).

[37] J. P. Carlo, J. P. Clancy, T. Aharen, Z. Yamani, J. P. C. Ruff, J. J. Wagman, G. J. Van Gastel, H. M. L. Noad, G. E. Granroth, J. E. Greedan, H. A. Dabkowska, and B. D. Gaulin, Phys. Rev. B **84**, 100404 (2011).

[38] Z. Qu, Y. Zou, S. Zhang, L. Ling, L. Zhang, and Y. Zhang, Journal of Applied Physics **113**, 170000 (2013), arXiv:1301.0383 [cond-mat.str-el].

[39] M. A. de Vries, J. O. Piatek, M. Misek, J. S. Lord, H. M. Rønnow, and J.-W. G. Bos, New Journal of Physics **15**, 043024 (2013), arXiv:1301.4982 [cond-mat.str-el].

[40] T. Aharen, J. E. Greedan, C. A. Bridges, A. A. Aczel, J. Rodriguez, G. MacDougall, G. M. Luke, V. K. Michaelis, S. Kroeker, C. R. Wiebe, H. Zhou, and L. M. D. Cranswick, Phys. Rev. B **81**, 064436 (2010).

[41] C. R. Wiebe, J. E. Greedan, P. P. Kyriakou, G. M. Luke, J. S. Gardner, A. Fukaya, I. M. Gat-Malureanu, P. L. Russo, A. T. Savici, and Y. J. Uemura, Phys. Rev. B **68**, 134410 (2003).

[42] C. R. Wiebe, J. E. Greedan, G. M. Luke, and J. S. Gardner, Phys. Rev. B **65**, 144413 (2002).

[43] K. Yamamura, M. Wakeshima, and Y. Hinatsu, J. Solid State Chem. **179**, 605 (2006).

[44] K. E. Stitzer, M. D. Smith, and H.-C. zur Loye, Solid State Sci. **4**, 311 (2002).

[45] A. S. Erickson, S. Misra, G. J. Miller, R. R. Gupta, Z. Schlesinger, W. A. Harrison, J. M. Kim, and I. R. Fisher, Phys. Rev. Lett. **99**, 016404 (2007).

[46] A. J. Steele, P. J. Baker, T. Lancaster, F. L. Pratt, I. Franke, S. Ghannadzadeh, P. A. Goddard, W. Hayes, D. Prabhakaran, and S. J. Blundell, Phys. Rev. B **84**, 144416 (2011).

[47] T. Aharen, J. E. Greedan, F. Ning, T. Imai, V. Michaelis, S. Kroeker, H. Zhou, C. R. Wiebe, and L. M. D. Cranswick, Phys. Rev. B **80**, 134423 (2009).

[48] G. A. Volovik, *The Universe in a Helium Droplet* (Oxford University Press, 2003).

[49] X. Wan, A. M. Turner, A. Vishwanath, and S. Y. Savrasov, Phys. Rev. B **83**, 205101 (2011).

[50] W. Witczak-Krempa and Y. B. Kim, Phys. Rev. B **85**, 045124 (2012).

[51] A. A. Burkov and L. Balents, Phys. Rev. Lett. **107**, 127205 (2011).

[52] X. Wan, A. Vishwanath, and S. Y. Savrasov, Phys. Rev. Lett. **108**, 146601 (2012).

[53] A. Go, W. Witczak-Krempa, G. S. Jeon, K. Park, and Y. B. Kim, Physical Review Letters **109**, 066401 (2012).

[54] B.-J. Yang and Y. B. Kim, Phys. Rev. B **82**, 085111 (2010).

[55] W. Witczak-Krempa, T. P. Choy, and Y. B. Kim, Phys. Rev. B **82**, 165122 (2010).

[56] G. Chen, R. Pereira, and L. Balents, Phys. Rev. B **82**, 174440 (2010).

[57] G. Chen and L. Balents, Phys. Rev. B **84**, 094420 (2011).

[58] T. Dodds, T.-P. Choy, and Y. B. Kim, Phys. Rev. B **84**, 104439 (2011).

[59] E.-G. Moon, C. Xu, Y. B. Kim, and L. Balents, arXiv preprint arXiv:1212.1168 (2012).

[60] C. Wang, A. C. Potter, and T. Senthil, Phys. Rev. B **88**, 115137 (2013); M. A. Metlitski, C. L. Kane, and M. P. A. Fisher, ArXiv e-prints (2013), arXiv:1306.3286 [cond-mat.str-el]; L. Fidkowski, X. Chen, and A. Vishwanath, Phys. Rev. X **3**, 041016 (2013); P. Bonderson, C. Nayak, and X.-L. Qi, Journal of Statistical Mechanics: Theory and Experiment **2013**, P09016 (2013).

[61] R. S. K. Mong, A. M. Essin, and J. E. Moore, Phys. Rev. B **81**, 245209 (2010).

[62] A. M. Turner, Y. Zhang, R. S. K. Mong, and A. Vishwanath, Phys. Rev. B **85**, 165120 (2012).

[63] T. L. Hughes, E. Prodan, and B. A. Bernevig, Phys. Rev. B **83**, 245132 (2011).

[64] C. Fang, M. J. Gilbert, and B. A. Bernevig, Phys. Rev. B **88**, 085406 (2013), arXiv:1304.6081 [cond-mat.mes-hall].

[65] M. Kargarian and G. A. Fiete, Phys. Rev. Lett. **110**, 156403 (2013).

[66] Z. Wang, X.-L. Qi, and S.-C. Zhang, Physical Review Letters **105**, 256803 (2010).

[67] Z. Wang, X.-L. Qi, and S.-C. Zhang, Phys. Rev. B **85**, 165126 (2012).

[68] Z. Wang and S.-C. Zhang, Physical Review X **2**, 031008 (2012), arXiv:1203.1028 [cond-mat.str-el].

[69] S. Murakami, New Journal of Physics **9**, 356 (2007).

[70] F. D. Haldane, Physical Review Letters **93**, 206602 (2004), arXiv:cond-mat/0408417.

[71] H. Nielsen and M. Ninomiya, Physics Letters B **130**, 389 (1983).

[72] G. Xu, H. Weng, Z. Wang, X. Dai, and Z. Fang, Phys. Rev. Lett. **107**, 186806 (2011).

[73] G. B. Halász and L. Balents, Phys. Rev. B **85**, 035103 (2012).

[74] T. Meng and L. Balents, Phys. Rev. B **86**, 054504 (2012).

[75] A. M. Turner and A. Vishwanath, arXiv preprint arXiv:1301.0330 (2013).

[76] O. Vafek and A. Vishwanath, ArXiv e-prints (2013), arXiv:1306.2272 [cond-mat.mes-hall].

[77] D. N. Sheng, Z.-C. Gu, K. Sun, and L. Sheng, Nature Communications **2**, 389 (2011), 10.1038/ncomms1380.

[78] T. Neupert, L. Santos, C. Chamon, and C. Mudry, Phys. Rev. Lett. **106**, 236804 (2011).

[79] E. Tang, J.-W. Mei, and X.-G. Wen, Phys. Rev. Lett. **106**, 236802 (2011).

[80] M. Kargarian, J. Wen, and G. A. Fiete, Phys. Rev. B **83**, 165112 (2011), arXiv:1101.0007 [cond-mat.str-el].

[81] Y. Machida, S. Nakatsuji, S. Onoda, T. Tayama, and T. Sakakibara, Nature **463**, 210 (2009).

[82] N. Taira, M. Wakeshima, and Y. Hinatsu, Journal of Physics: Condensed Matter **13**, 5527+ (2001).

[83] H. Fukazawa and Y. Maeno, Journal of the Physical Society of Japan **71**, 2578 (2002).

[84] K. Matsuhira, M. Wakeshima, Y. Hinatsu, and S. Takagi, Journal of the Physical Society of Japan **80**, 094701 (2011).

[85] T. Hasegawa, N. Ogita, K. Matsuhira, S. Takagi, M. Wakeshima, Y. Hinatsu, and M. Udagawa, Journal of Physics: Conference Series **200**, 012054 (2010).

[86] S. Zhao, J. M. Mackie, D. E. MacLaughlin, O. O. Bernal, J. J. Ishikawa, Y. Ohta, and S. Nakatsuji, Phys. Rev. B **83**, 180402 (2011).

[87] J. J. Ishikawa, E. C. T. O'Farrell, and S. Nakatsuji, Phys. Rev. B **85**, 245109 (2012).

[88] K. Tomiyasu, K. Matsuhira, K. Iwasa, M. Watahiki, S. Takagi, M. Wakeshima, Y. Hinatsu, M. Yokoyama, K. Ohoyama, and K. Yamada, Journal of the Physical Society of Japan **81**, 034709+ (2012).

[89] F. F. Tafti, J. J. Ishikawa, A. McCollam, S. Nakatsuji, and S. R. Julian, Phys. Rev. B **85**, 205104 (2012).

[90] M. Sakata, T. Kagayama, K. Shimizu, K. Matsuhira, S. Takagi, M. Wakeshima, and Y. Hinatsu, Phys. Rev. B **83**, 041102 (2011).

[91] M. C. Shapiro, S. C. Riggs, M. B. Stone, C. R. de la Cruz, S. Chi, A. A. Podlesnyak, and I. R. Fisher, Phys. Rev. B **85**, 214434 (2012).

[92] S. M. Disseler, C. Dhital, T. C. Hogan, A. Amato, S. R. Giblin, C. de la Cruz, A. Daoud-Aladine, S. D. Wilson, and M. J. Graf, Phys. Rev. B **85**, 174441 (2012).

[93] S. M. Disseler, C. Dhital, A. Amato, S. R. Giblin, C. de la Cruz, S. D. Wilson, and M. J. Graf, Phys. Rev. B **86**, 014428 (2012).

[94] H. Sagayama, D. Uematsu, T. Arima, K. Sugimoto, J. J. Ishikawa, E. O'Farrell, and S. Nakatsuji, Phys. Rev. B **87**, 100403 (2013).

[95] M. Subramanian, G. Aravamudan, and G. S. Rao, Progress in Solid State Chemistry **15**, 55 (1983).

[96] H.-J. Koo, M.-H. Whangbo, and B. Kennedy, Journal of Solid State Chemistry **136**, 269 (1998).

[97] H. Guo, K. Matsuhira, I. Kawasaki, M. Wakeshima, Y. Hinatsu, I. Watanabe, and Z.-a. Xu, Phys. Rev. B **88**, 060411 (2013), arXiv:1308.3283 [cond-mat.str-el].

[98] W. Witczak-Krempa, A. Go, and Y. B. Kim, Phys. Rev. B **87**, 155101 (2013).

[99] M. Kurita, Y. Yamaji, and M. Imada, Journal of the Physical Society of Japan **80**, 044708+ (2011).

[100] A. Go, W. Witczak-Krempa, G. S. Jeon, and Y. B. Kim, (in preparation).

[101] W. Witczak-Krempa and Y. B. Kim, (unpublished).

[102] K.-Y. Yang, Y.-M. Lu, and Y. Ran, Phys. Rev. B **84**, 075129 (2011).

[103] H. B. Nielsen and M. Ninomiya, Physics Letters B **130**, 389 (1983).

[104] G. Kotliar, S. Y. Savrasov, K. Haule, V. S. Oudovenko, O. Parcollet, and C. A. Marianetti, Rev. Mod. Phys. **78**, 865 (2006).

[105] T. Maier, M. Jarrell, T. Pruschke, and M. H. Hettler, Rev. Mod. Phys. **77**, 1027 (2005).

[106] S. Nakatsuji, Y. Machida, Y. Maeno, T. Tayama, T. Sakakibara, J. v. Duijn, L. Balicas, J. N. Millican, R. T. Macaluso, and J. Y. Chan, Phys. Rev. Lett. **96**, 087204 (2006).

[107] Y. Machida, S. Nakatsuji, Y. Maeno, T. Tayama, T. Sakakibara, and S. Onoda, Phys. Rev. Lett. **98**, 057203 (2007).

[108] S. Onoda and Y. Tanaka, Phys. Rev. Lett. **105**, 047201 (2010).

[109] S. Onoda and Y. Tanaka, Phys. Rev. B **83**, 094411 (2011).

[110] R. Flint and T. Senthil, Phys. Rev. B **87**, 125147 (2013), arXiv:1301.0815 [cond-mat.str-el].

[111] S. Lee, A. Paramekanti, and Y. B. Kim, ArXiv e-prints (2013), arXiv:1305.0827 [cond-mat.str-el].

[112] G. Chen and M. Hermele, Phys. Rev. B **86**, 235129 (2012).

[113] K. Ueda, J. Fujioka, Y. Takahashi, T. Suzuki, S. Ishiwata, Y. Taguchi, and Y. Tokura, Phys. Rev. Lett. **109**, 136402 (2012).

[114] E. K.-H. Lee, S. Bhattacharjee, and Y. B. Kim, Phys. Rev. B **87**, 214416 (2013), arXiv:1210.5242 [cond-mat.str-el].

[115] K. I. Kugel and D. I. Khomskii, Sov. Phys. Usp. **25**, 231 (1982).

[116] H. Jahn and E. Teller, Proc. R. Soc. Lond. A **161**, 220 (1937).

[117] G. Jackeli and G. Khaliullin, Physical review letters **102**, 017205 (2009).

[118] Annals of Physics **321**, 2 (2006).

[119] J. Chaloupka, G. Jackeli, and G. Khaliullin, Phys. Rev. Lett. **105**, 027204 (2010).

[120] J. Chaloupka, G. Jackeli, and G. Khaliullin, Phys. Rev. Lett. **110**, 097204 (2013).

[121] G. Chen and L. Balents, Phys. Rev. B **78**, 094403 (2008).

[122] I. I. Mazin, H. O. Jeschke, K. Foyevtsova, R. Valentí, and D. I. Khomskii, Phys. Rev. Lett. **109**, 197201 (2012).

[123] J. Reuther, R. Thomale, and S. Trebst, Phys. Rev. B **84**, 100406 (2011).

[124] I. Kimchi and Y.-Z. You, Phys. Rev. B **84**, 180407 (2011).

[125] S. Bhattacharjee, S.-S. Lee, and Y. B. Kim, New Journal of Physics **14**, 073015 (2012).

[126] J. Reuther, R. Thomale, and S. Rachel, Phys. Rev. B **86**, 155127 (2012), arXiv:1206.3103 [cond-mat.str-el].

[127] J. B. Goodenough, Phys. Rev. **171**, 466 (1968).

[128] A. Läuchli, F. Mila, and K. Penc, Phys. Rev. Lett. **97**, 087205 (2006).

[129] I. Affleck, T. Kennedy, E. Lieb, and H. Tasaki, Communications in Mathematical Physics **115**, 477 (1988).

[130] S. Sachdev, Annales Henri Poincaré **4**, 637 (2003).

[131] K. W. Lee and W. Pickett, Europhys. Lett. **80**, 37008 (2007).

[132] H. J. Xiang and M.-H. Whangbo, Phys. Rev. B **75**, 052407 (2007).

[133] P. Santini, S. Carretta, G. Amoretti, R. Caciuffo, N. Magnani, and G. H. Lander, Rev. Mod. Phys. **81**, 807 (2009).

[134] R. Shiina, O. Sakai, H. Shiba, and P. Thalmeier, Journal of the Physical Society of Japan **67**, 941 (1998).

[135] J.-M. Carter and H.-Y. Kee, Phys. Rev. B **87**, 014433 (2013).

[136] M. A. Zeb and H.-Y. Kee, Phys. Rev. B **86**, 085149 (2012).

[137] J.-M. Carter, V. V. Shankar, M. A. Zeb, and H.-Y. Kee, Phys. Rev. B **85**, 115105 (2012).

[138] O. B. Korneta, T. Qi, S. Chikara, S. Parkin, L. E. De Long, P. Schlottmann, and G. Cao, Phys. Rev. B **82**, 115117 (2010).

[139] T. F. Qi, O. B. Korneta, L. Li, K. Butrouna, V. S. Cao, X. Wan, P. Schlottmann, R. K. Kaul, and G. Cao, Phys. Rev. B **86**, 125105 (2012).

[140] S. Calder, G.-X. Cao, M. D. Lumsden, J. W. Kim, Z. Gai, B. C. Sales, D. Mandrus, and A. D. Christianson, Phys. Rev. B **86**, 220403 (2012).

[141] F. Wang and T. Senthil, Physical Review Letters **106**, 136402 (2011).

[142] Y.-Z. You, I. Kimchi, and A. Vishwanath, Phys. Rev. B **86**, 085145 (2012).

[143] S. Okamoto, Physical Review Letters **110**, 066403 (2013), arXiv:1210.2290 [cond-mat.str-el].

[144] M. Levin and A. Stern, Phys. Rev. Lett. **103**, 196803 (2009).

[145] J. Maciejko, X.-L. Qi, A. Karch, and S.-C. Zhang, Phys. Rev. B **86**, 235128 (2012).

[146] B. Swingle, M. Barkeshli, J. McGreevy, and T. Senthil, Phys. Rev. B **83**, 195139 (2011).

[147] P. Coleman and A. J. Schofield, Nature (London) **433**, 226 (2005).

[148] R. Comin, G. Levy, B. Ludbrook, Z.-H. Zhu, C. N. Veenstra, J. A. Rosen, Y. Singh, P. Gegenwart, D. Stricker, J. N. Hancock, D. van der Marel, I. S. Elfimov, and A. Damascelli, Phys. Rev. Lett. **109**, 266406 (2012).

[149] D. Hsieh, F. Mahmood, D. Torchinsky, G. Cao, and N. Gedik, Physical Review B **86**, 035128 (2012).

[150] L. de' Medici, X. Wang, M. Capone, and A. J. Millis, Phys. Rev. B **80**, 054501 (2009).

[151] K. Foyevtsova, H. O. Jeschke, I. I. Mazin, D. I. Khomskii, and R. Valentí, Phys. Rev. B **88**, 035107 (2013), arXiv:1303.2105 [cond-mat.str-el].

[152] I. I. Mazin, S. Manni, K. Foyevtsova, H. O. Jeschke, P. Gegenwart, and R. Valentí, Phys. Rev. B **88**, 035115 (2013), arXiv:1304.2258 [cond-mat.str-el].

[153] D. Xiao, W. Zhu, Y. Ran, N. Nagaosa, and S. Okamoto, Nature Communications **2**, 596 (2011), 10.1038/ncomms1602, arXiv:1106.4296 [cond-mat.mtrl-sci].

[154] F. Wang and Y. Ran, Phys. Rev. B **84**, 241103 (2011).

[155] X. Hu, A. Rüegg, and G. A. Fiete, Phys. Rev. B **86**, 235141 (2012).